From Sensing to Action: A Leaf Humidity–Triggered Closed Loop System for Precision Salicylic Acid Delivery to Mitigate Plant Stress

Rhythem Tahrin
The University of Texas at Tyler
Sean C. Butler
The University of Texas at Tyler
Shawana Tabassum
stabassum@uttyler.edu

The University of Texas at Tyler

Article

Keywords: Precision plant healthcare, Leaf humidity sensing, Salicylic acid, Thermoresponsive hydrogel, Closed loop system, Biomolecule release modeling

Posted Date: June 8th, 2026

DOI: https://doi.org/10.21203/rs.3.rs-9800573/v1

Additional Declarations: No competing interests reported.

From Sensing to Action: A Leaf Humidity–Triggered Closed Loop System for Precision Salicylic Acid Delivery to Mitigate Plant Stress

Rhythem Tahrin[1], Sean C. Butler[2], and Shawana Tabassum[1*]

[1]Department of Electrical Engineering, The University of Texas at Tyler, Tyler, TX

[2]Department of Chemistry and Biochemistry, The University of Texas at Tyler, Tyler, TX

*Corresponding author: stabassum@uttyler.edu

Abstract

Real-time detection of plant stress and timely delivery of protective biomolecules are essential for improving crop resilience under adverse environmental conditions. However, conventional plant monitoring systems typically rely on ambient measurements and passive treatment strategies that fail to enable targeted plant recovery based on their localized physiological conditions. As a result, current approaches largely operate as open-loop systems, where sensing and intervention are not directly integrated, limiting the ability to respond dynamically to plant stress. This study presents an integrated plant healthcare platform that bridges this gap by combining leaf-level humidity sensing with stimulus-responsive delivery of the phytohormone salicylic acid (SA) to enable a closed-loop plant care system. The objective of this work was to develop a platform capable of monitoring transpiration driven humidity changes at the leaf surface and enabling controlled hormone delivery based on plant physiological responses. A temperature responsive hydrogel encapsulating SA was synthesized to achieve sustained biomolecule release while minimizing initial burst release. Salicylic acid release kinetics were evaluated using multiple mathematical models, with the Korsmeyer–Peppas model providing the best fit ($R^2 = 0.9978$), indicating that SA release was governed primarily by polymer relaxation and degradation mechanisms. Leaf-level relative humidity was continuously monitored on the abaxial surface under different treatment conditions. Plants treated with the hydrogel-based SA delivery system showed improved drought tolerance, with localized relative humidity increasing from approximately 20–30% in stressed plants to 60–70% after treatment, while untreated stressed plants did not show any noticeable recovery. This improvement was further supported by measurements of stomatal aperture, which showed a mean opening of 1.932 micrometers in treated plants, compared to 0.396 micrometers in untreated plants. SA treated seeds also demonstrated accelerated germination within 14 days. These findings demonstrate the potential of integrating plant wearable sensors with stimulus responsive biomaterials to establish closed-loop plant healthcare systems that couple physiological sensing with adaptive intervention.

Keywords: Precision plant healthcare, Leaf humidity sensing, Salicylic acid, Thermoresponsive hydrogel, Closed loop system, Biomolecule release modeling.

1. Introduction

The world population is projected to reach 11.2 billion by 2100, significantly increasing global food demand [1]. However, cultivable land is expected to shrink due to urbanization and environmental degradation. In parallel, rising carbon emissions and global warming are intensifying environmental stressors, particularly drought, which lead to water scarcity in plants and a sharp decline in agricultural productivity [2]. These abiotic stressors impair vital physiological processes in plants, most notably transpiration, which governs water movement and gas exchange through the stomata [3]. Under normal conditions, healthy plants exhibit high transpiration rates, releasing water vapor that influences the surrounding relative humidity (RH). However, environmental stress prompts stomatal closure, suppressing transpiration and reducing humidity in the leaf microclimate. This phenomenon creates an opportunity to infer plant stress through RH measurements [4]. Despite these advances, current technologies lack the capability to monitor leaf microclimate in real time and to enable controlled, efficient delivery of biomolecules for mitigating plant stress under dynamic environmental conditions [5].

To enhance plant resilience, researchers have investigated the external application of biomolecules like salicylic acid (SA) using delivery approaches such as foliar sprays and hydrogel systems. SA is a critical plant hormone involved in growth, development, and defense. It plays a key role in modulating stomatal function, photosynthesis, and nutrient uptake, while also acting as a central signaling molecule in systemic acquired resistance (SAR) [6]. SA interacts with other hormonal pathways such as jasmonic acid and abscisic acid to coordinate stress responses, and activates defense related genes like pathogenesis related (PR) proteins [6]. SA boosts the activities of key antioxidative enzymes such as peroxidase (POD), polyphenol oxidase (PPO), and superoxide dismutase (SOD), mitigating oxidative stress and promoting plant health during drought, salinity, or extreme temperatures [7]. During biotic stress, SA levels naturally rise in response to pathogen attacks. However, prior work demonstrated that excessive drought conditions can suppress SA biosynthesis in plants [5,8,9]. Therefore, when endogenous SA production is insufficient, external application of SA has proven to be an effective strategy to enhance plant defense and significantly improve crop yield under stress conditions. For instance, foliar spraying of 0.75 mM SA on French beans under salt stress restored up to 90% of control yield [10]. In cold stressed maize plants, 0.5 mM SA enhanced growth rate under hydroponic conditions [11]. Exogenous application further enhances defense by activating PR genes and secondary metabolite pathways. For example, SA treated watermelon plants showed increased resistance to cucumber green mottle mosaic virus (CGMMV) through elevated flavonoid biosynthesis [12], while another study showed that SA inhibited Rice Black Streaked Dwarf Virus (RBSDV) infection in rice [13]. In tomato plants, passive delivery of SA via nanomaterials increased SA levels by up to 45%, enhancing resistance to fungal infection [14]. SA also confers general physiological benefits, including improved germination, flowering, and biomass production across species [15]. In Butterhead Lettuce, slow release of SA increased root mass and enhanced plant immunity [16]. In wheat, SA improved antioxidant activity and shoot root growth metrics [17], while in *Catharanthus roseus* it upregulated drought tolerant genes and boosted carotenoid, alkaloid, and chlorophyll content [18]. Furthermore, synergistic effects are seen when SA is combined with other hormones. In soybeans, for example, the combination of SA and GA3 improved pod development and chlorophyll retention under waterlogged conditions [19].

Despite its broad benefits, SA's success depends on precise delivery at critical growth stages. Traditional foliar spraying is prone to degradation, poor uptake, and lack of delivery control, particularly under stress conditions [10,20,21]. To address these challenges, hydrogel based systems

have been developed to enable controlled release, but many rely on passive degradation mechanisms and lack the structural adaptability required for precise or localized delivery [22,23]. Furthermore, several hydrogel designs fail to align release rates with the dynamic physiological needs of the plant. For example, bulk hydrogels used in earlier studies demonstrated slow but uncontrolled degradation and release profiles [24,25]. Additionally, some systems fail to deliver SA at the right stage of plant development or in response to environmental cues, leading to waste and limited therapeutic efficacy [15,26]. In a preliminary work, our group presented a three-dimensional (3D) printed thermo-responsive hydrogel actuator for controlled release of SA [27]. The system enabled sustained and localized delivery of SA through a temperature-triggered mechanism, and demonstrated improved structural adaptability compared to conventional bulk hydrogels. However, the actuator operated as a passive delivery platform, where release was governed solely by environmental temperature without incorporating real-time feedback from the plant. As a result, the system lacked the ability to dynamically adjust SA delivery based on the plant's physiological state or stress level. Furthermore, it did not include any sensing capability to monitor leaf-level microclimate conditions, which are critical indicators of early stress responses. These limitations highlight the need for an integrated platform that can both detect plant stress in real time and actively regulate biomolecule delivery in response to those signals. Therefore, despite ongoing research, current hydrogel based delivery platforms still face major challenges in achieving precision, responsiveness, and sustainability in agricultural applications [28].

Transpiration is governed by the leaf microclimate, particularly the RH at the stomatal interface, which directly controls vapor pressure deficit (VPD) and water loss. Because early drought stress manifests as subtle changes in leaf level humidity before visible symptoms appear, real time monitoring of leaf RH is critical for timely intervention [4,5]. Conventional humidity sensors positioned in ambient air or soil provide indirect measurements and fail to capture the dynamic microclimate at the leaf surface, often delaying stress detection due to environmental noise and poor spatial resolution. To overcome these limitations, recent studies have introduced flexible, conformable, and miniaturized leaf sensors capable of directly measuring RH, temperature, and VPD at the leaf surface [29]. Other studies employed adhesive mounted configurations that maintain a breathable air gap, preventing stomatal blockage [5,30]. Our group previously reported a multifunctional, flexible patch that integrates temperature, RH, and hormone sensors on the leaf surface [5,8,31]. Oren et al. developed a low cost, flexible graphene-based humidity sensor transferred onto adhesive tapes using a peel transfer method. The patch was mounted on plant leaves for water transport monitoring, with the sensor coating made of multilayer graphene nanoplatelets [32]. Lee et al. designed a multimodal sensor patch mounted on the abaxial leaf surface to monitor volatile organic compounds, temperature, and humidity [33]. These systems including graphene based, carbon nanotube–based, and polymer composite sensing platforms have demonstrated improved sensitivity to stomatal microclimate dynamics. While these advances represent an important step toward precision plant monitoring, existing platforms largely function as passive diagnostic tools. They report environmental or physiological data but do not translate those signals into actionable interventions. To date, although several studies have reported leaf mounted humidity sensors, none have utilized real time leaf humidity data to actively trigger a therapeutic response, such as targeted biomolecule delivery, to mitigate the plant stress conditions.

Our research addresses this critical gap by integrating a leaf humidity based stress diagnostic platform with a responsive SA delivery mechanism, thereby establishing a true closed loop plant care system. At its core is a thermoresponsive hydrogel engineered to release SA near 32°C [34], which is closely aligned with physiological stress conditions in plants [35]. This threshold is critical,

as temperatures above 30–32 °C can disrupt transpiration, photosynthesis, and hormone signaling pathways, thereby triggering the need for protective responses for stress mitigation [36]. Unlike conventional bulk hydrogels, which lack structural flexibility, the hydrogel films developed in this study can be directly applied to leaf surfaces or soil, enabling targeted, localized delivery and improved adaptability to changing environmental conditions. This customizable release system ensures sustained SA delivery while minimizing chemical waste, enhancing precision agriculture applications. A key innovation of this work is the integration of real time leaf level RH monitoring with adaptive biomolecule delivery, forming a fully integrated closed loop system. A flexible sensor developed in our earlier work is mounted on the abaxial surface of leaves to monitor RH as an indicator of stomatal activity and transpiration-driven plant water stress [37]. When stress is detected, SA is delivered to the plant, promoting hormone assisted recovery and mitigating drought induced physiological decline. As shown in Figure 1, this feedback loop continuously monitors RH and delivers SA, enabling plants to dynamically respond to evolving stress conditions. By synchronizing physiological sensing with adaptive biomolecule delivery, our system closes the feedback loop between stress detection and intervention. This enables precise temporal control of SA delivery, minimizes unnecessary chemical application, and supports plant specific, point of care decision making directly at the leaf interface. Ultimately, this approach transforms leaf humidity monitoring from a passive measurement tool into an active, intelligent strategy for real time mitigation of plant water stress.

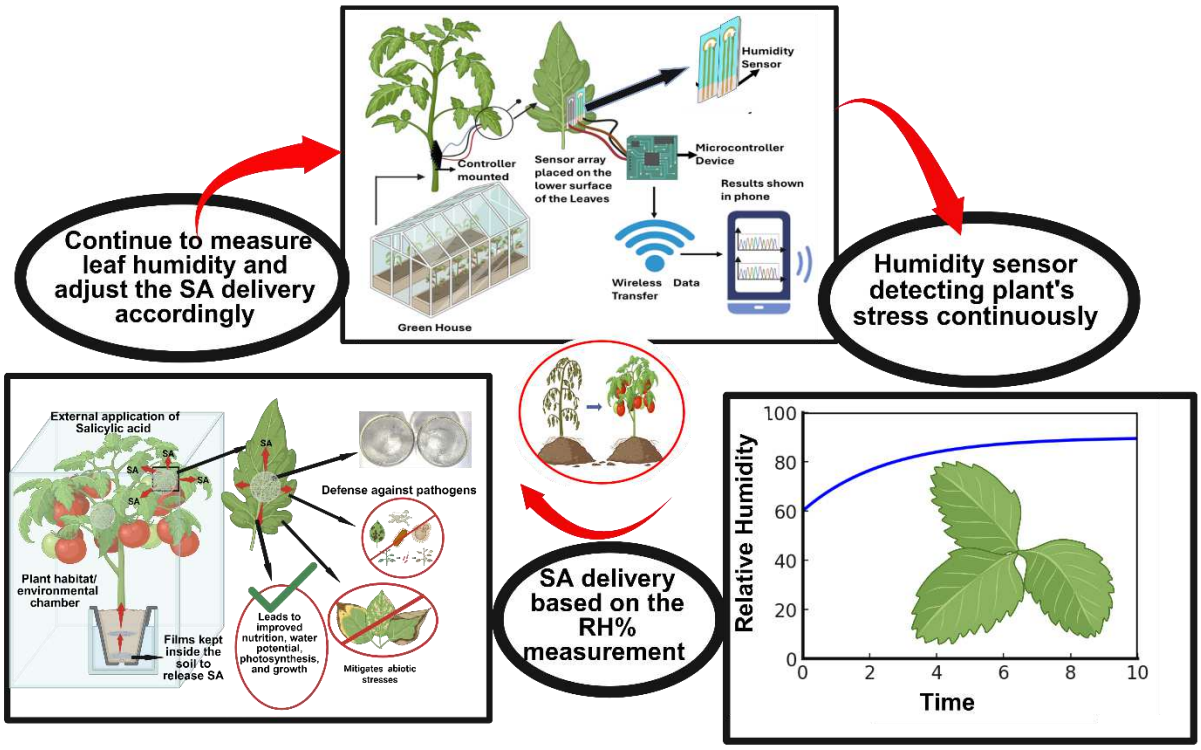

Figure 1: Closed loop feedback system for adaptive SA delivery via humidity sensing in leaves.

The key innovations of this work include:

- Applying a flexible humidity sensor to monitor leaf-level RH in response to water stress [37].
- Engineering stimulus responsive hydrogel capable of controlled, sustained delivery of SA on demand.
- Integrating the sensor and hydrogel system into an adaptive platform for proactive, personalized plant stress mitigation.

2. Materials and Methods

2.1 In Vitro Hormone Release Studies for Hydrogel Optimization

The hydrogel-based delivery system consists of a thermoresponsive polymer network composed of salicylic acid–based poly(anhydride ester) (SAPAE) integrated within a poly(*N*-isopropylacrylamide) (PNIPAAM) matrix for controlled SA release. SAPAE serves as a biodegradable biomolecule system in which SA molecules are chemically incorporated into the polymer backbone and are released through hydrolytic degradation of anhydride and ester bonds under aqueous conditions [38]. This mechanism enables sustained and localized delivery of SA, minimizing burst release and improving therapeutic efficiency. PNIPAAM, a temperature-sensitive polymer, exhibits a lower critical solution temperature (LCST) near 32 °C, above which the polymer undergoes a hydrophilic-to-hydrophobic transition, leading to network collapse and triggered release of the encapsulated biomolecule. Together, the SAPAE–PNIPAAM system forms a hybrid hydrogel platform that integrates both degradation-controlled and stimulus-responsive release mechanisms. Such hydrogel systems typically possess a 3D-crosslinked network structure that allows high water absorption while maintaining structural integrity, thereby enabling controlled diffusion of encapsulated agents [39]. This synergistic release behavior provides enhanced temporal control over SA delivery, making the platform well suited for applications requiring sustained and environmentally responsive hormone release.

The synthesis procedure of the hydrogel system is detailed in **Supporting Information A**. To determine the optimized hydrogel formulation for SA release, four samples (A, B, C and D, as detailed in **Supporting Information A.3**) were prepared and evaluated through in vitro release studies. The hydrogel samples were placed inside capped bottles, which were subsequently kept in a water bath to investigate the release kinetics of SA (Figure 2). Because PNIPAAM undergoes a phase transition near its LCST of ~32 °C [40], the water bath temperature was maintained above 32 °C to ensure accurate and consistent release measurements. Phosphate-buffered saline (PBS) was used as the release medium to provide a physiologically relevant dissolution environment. At predetermined time intervals, a fixed volume of the release medium was carefully withdrawn from each sample with minimal disturbance to the hydrogel structure, and an equal volume of fresh PBS was replenished to maintain constant solution volume. The collected samples were then analyzed using UV-Vis spectrophotometry at 295.5 nm wavelength to quantify SA concentration [41], based on a pre-established calibration curve (**Supporting Information B.1**). In addition, detailed morphological and chemical characterization of the synthesized hydrogels is presented in **Supporting Information B.2.**

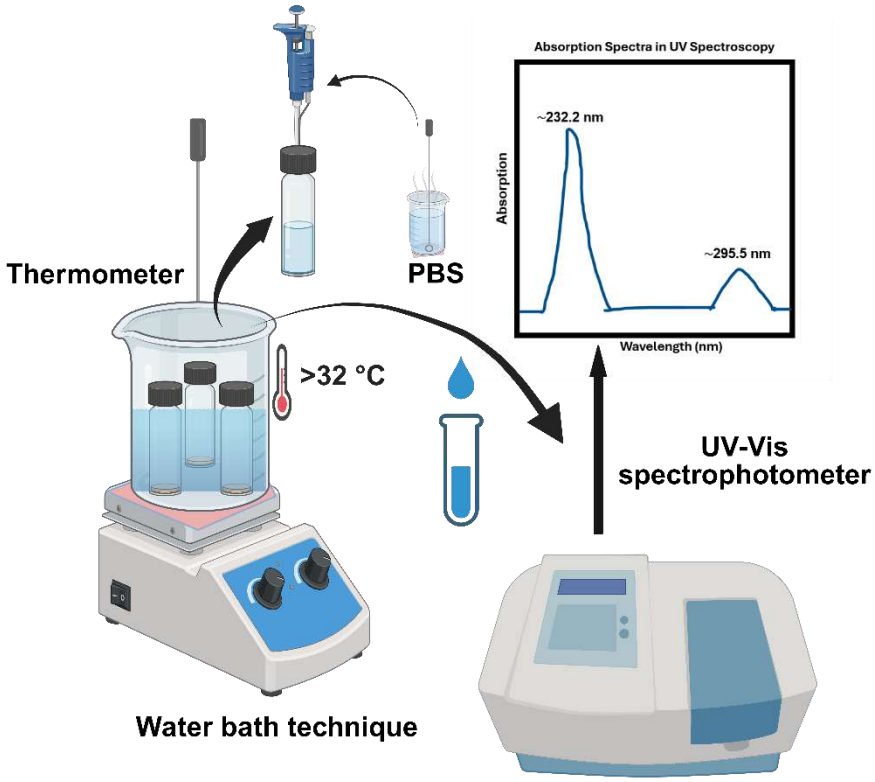

Figure 2: Experimental setup for in vitro hormone release test.

2.2 Kinetic Model Fitting of Experimental SA Release Data

To evaluate the SA release mechanisms from the prepared hydrogel samples (A, B, C, and D), the release kinetics of SA from each formulation were analyzed using multiple mathematical models, as detailed in **Supporting Information C**. These included the zero-order, first-order, Higuchi, Hixson–Crowell, and Korsmeyer–Peppas models, which collectively describe diffusion-controlled, surface erosion–driven, and polymer relaxation–mediated release behaviors. Experimental cumulative release data obtained from UV–Vis analysis were fitted to each model, and the goodness of fit was assessed using correlation coefficients (R^2 values). The Korsmeyer–Peppas model was further applied to the initial 60% of release data to determine the dominant release mechanism through the release exponent (n) and rate constant (k). In addition, key kinetic parameters such as time of release and maximum cumulative release were also analyzed to compare formulation performance.

2.3 Experimental Design for Studies on Grown Plants

A total of 12 fully matured bell pepper plants (*Capsicum annuum*) were purchased from Lowe's Garden Center in Tyler, Texas. These plants were divided into four groups, each having three plants (Table 1). The plants were first rehydrated following transport, and experimental observations began two days later. These two days acclimatization period was provided to allow the plants to recover from transplant shock and physiological stress induced by transport and

changes in environmental conditions such as light, humidity, and temperature. Such a stabilization phase ensures that the collected data reflects plant responses under steady state conditions rather than transient stress effects. During the acclimatization period, the plants were kept in controlled laboratory conditions with a temperature range of approximately 23–25 °C and RH maintained between 45–55%. Following the first day of data collection, the plants were placed outdoors under direct sunlight during the day to simulate natural environmental conditions. To simulate drought conditions, irrigation was withheld for the first five to six days until the RH level dropped significantly for all groups except the control group that were watered daily (Group 4). Data acquisition was conducted indoors each morning.

Leaf level RH for each plant was measured daily over a 10-day period, with each recording lasting 20 minutes using commercial multimeters (Hewlett-Packard, Palo Alto, CA, USA), as illustrated in Figure 3. It is well understood that plant leaves do not have an intrinsic RH; rather, they contribute to the surrounding microenvironment's humidity through transpiration, the process by which water vapor exits the leaf through stomatal pores. A healthy plant typically exhibits higher transpiration rates, releasing more water vapor to the surrounding air. During water deficit conditions, plants typically respond by closing their stomata to conserve water, which leads to a reduction in transpiration rate and subsequently lowers the humidity immediately surrounding the leaf surface [42–44]. To more precisely capture localized humidity variations, custom-fabricated humidity sensors [37] were mounted on the abaxial surface of bell pepper leaves. The sensors were affixed using 20 μm-thick double-sided tape applied only along the edges (~1 mm width), ensuring that the active sensing region was exposed to the stomatal surface. This 20 μm gap between the leaf and sensing surface avoided obstruction of stomata. The resulting configuration enabled continuous, high-resolution monitoring of humidity directly at the leaf surface.

Once leaf RH measurements indicated a significant and sustained decline interpreted as a drought-induced stress response due to reduced transpiration, hormone loaded films (SAPAE-PNIPAAM or SA- PNIPAAM) were applied at the root zone within the soil. For this application, the films were prepared in 11 mm diameter, 2 mL glass vials. The smaller size and lower volume were chosen to enhance root uptake efficiency of the released SA. These 2 mL vials were inserted into the soil near the plant roots, facilitating easier hormone absorption under simulated drought conditions (Figure 4).

Table 1: Description of Plant Groups and Assigned Treatments

Group Name	Treatment	No of plants
Group 1	Treated with SAPAE encapsulated PNIPAAM hydrogel films upon showing stress (SAPAE-PNIPAAM)	3
Group 2	Treated with SA encapsulated PNIPAAM hydrogel films upon showing stress (SA- PNIPAAM)	3
Group 3	Drought stressed plants without any hormone treatment	3
Group 4	Regular watering throughout the experiment to maintain healthy conditions (true control)	3

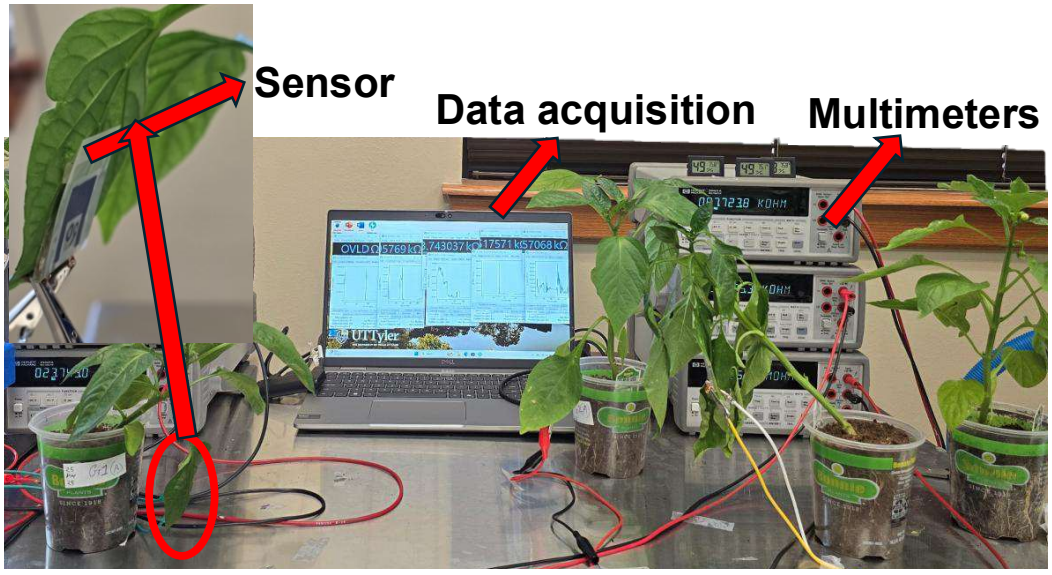

Figure 3: Experimental setup for real time sensing and SA delivery in grown plants.

Figure 4: Experimental setup for testing the SA delivery in full grown bell pepper plants. Left: Hormone loaded hydrogel films cast into 2 mL glass vials. Right: A SAPAE film loaded vial placed at the root zone of a potted plant to enable hormone uptake following stress detection via leaf mounted RH sensors.

At the end of the 10-day experiment, images of the plant canopy were captured to qualitatively assess plant recovery characteristics, including leaf turgor, upright posture, and overall plant vitality under drought stress conditions. A high-resolution digital camera (Sony Alpha a6000 Mirrorless Digital Camera, Sony Corporation, Tokyo, Japan) was used to record these images. After canopy imaging, the plants were carefully uprooted from the containers, and the root areas were gently cleaned to remove adhered soil. Root images were then acquired to evaluate root

morphology, including vertical root length and lateral root spread. The obtained measurements were used for quantitative comparison of overall root development among the treated plants.

To quantify stomatal aperture differences among treatment groups, scanning electron microscopy (SEM) images of stomata from the abaxial side of the leaf were analyzed following the 10-day experiment. For each treatment group, the aperture lengths of 10 individual stomata were measured using ImageJ software (ImageJ, National Institutes of Health, USA), and the corresponding mean and standard deviation values were calculated. This analysis provided a quantitative comparison of stomatal behavior across different treatments and stress conditions, complementing the qualitative observations from SEM imaging.

2.4 Experimental Design for Studies on Seeds

To evaluate the potential physiological effects of SA and SAPAE on plant development, a series of germination and early growth experiments were conducted using tomato and bell pepper seeds under controlled conditions. All seeds were procured from Lowe's Garden Center (Tyler, TX, USA). In the first experiment (Phase 1), tomato (*Solanum lycopersicum*, Roma VF) seeds were grown in 20 mL glass bottles (28 mm diameter) containing soil. Three experimental groups were prepared (Table 2, Phase 1), with the inner surfaces of the bottles pre-coated using different hydrogel film formulations (Table A.1, Supporting Information). Each bottle served as an individual pot and was maintained in a drought stressed condition with intermittent watering over a 14-day period. All samples were incubated in an artificial environmental chamber to ensure a consistent temperature of 35 ºC, a humidity level of 30%, and two-sided lighting illumination of 6000 lux. Seed germination rate and early growth responses were visually monitored and recorded. To enable controlled hormone release, water was intermittently introduced through a small inlet at the bottom of each bottle. This design promoted capillary-driven flow toward the hormone-loaded film, enabling potential hormone release upon exposure to moisture. The temperature of the irrigation water was maintained above the LCST of PNIPAAM to trigger its thermoresponsive deswelling behavior, thereby facilitating the on-demand release of SA. This experimental design ensured that hormone diffusion was thermally activated and spatially localized near the seed, allowing for precise evaluation of hormone induced germination and early seedling growth under abiotic stress.

To further validate the effectiveness of SAPAE films as a hormone delivery system, a second seedling growth study was conducted using bell pepper (*Capsicum annuum*) seeds over a 14-day period. The experiment included replicated pots for each treatment condition, along with a true control group that received neither drought stress nor hormonal treatment. During this phase, four experimental groups were set up, with each group comprising three separate pots, each containing a single seed (Table 2, Phase 2). This phase aimed to evaluate both seed germination and early-stage seedling responses to sustained hormonal exposure under abiotic stress. A laboratory environment was selected to enable close monitoring and maintain consistent conditions as an alternative to a programmable environmental chamber. Under these conditions, ambient RH ranged from 45% to 55%, while pot temperatures were maintained at 35 °C using a water bath setup. This thermal setup was chosen to mimic heat-induced drought conditions, similar to the previous tomato seed experiment. All treatment pots were irrigated intermittently using warm water delivered through a small aperture in the bottle, ensuring that water temperature remained

above the LCST of PNIPAAM. This condition enabled thermally triggered, localized release of SA from the polymeric matrix.

The primary objective of these experiments was to assess the comparative effectiveness of SAPAE based sustained hormone delivery versus free SA application in promoting germination and early growth under abiotic stress. This study offers a controlled framework for evaluating how release kinetics, hormone form and external stressors influence early plant development. Results from these experiments will inform the broader potential of SAPAE based systems in agriculture and stress tolerant plant engineering.

Table 2: Description of Seed Treatment Groups for Phases 1 and 2

	Group Name	Treatments	No of seeds
Phase 1 with tomato	Group 1	Bottles coated with SAPAE-PNIPAAM under drought stress	1
	Group 2	Bottles coated with SA-PNIPAAM under drought stress	1
	Group 3	Bottles coated with no SA treatment under drought stress	1
Phase 2 with bell pepper	Group 1	Bottles coated with SAPAE-PNIPAAM under drought stress	3
	Group 2	Bottles coated with SA-PNIPAAM under drought stress	3
	Group 3	Bottles coated with no SA treatment under drought stress	3
	Group 4	Regular watering without any hormone application (true control)	3

3. Results and Discussion

3.1 Experimental SA Release Kinetics

Figure 5 represents the cumulative SA release profiles of samples A, B, C, and D (Table A.1, Supporting Information), highlighting the impact of formulation composition and mechanical handling on SA release behavior. Since samples A and B were compositionally identical, the variations in their release behavior stem primarily from mechanical handling differences during the water bath sampling process (Figure 2). Sample A, which was subjected to frequent sampling, exhibited a moderate release profile, reaching approximately 66% of the SA release at 174 hr. However, this lower cumulative release was not necessarily due to intrinsic diffusion limitations but rather due to mechanical degradation. During each sampling interval, the film was physically removed from the water bath and reintroduced, leading to structural weakening and breakage over time. Small fragments of the broken polymer film were likely lost during sampling, particularly when the solution was extracted for UV-Vis spectroscopy analysis. This loss of polymeric material would have removed some of the encapsulated SA, artificially lowering the measured cumulative release. Sample B, which was sampled less frequently, exhibited the most sustained and extended release, reaching 99.5% SA release at 191 hr. The reduced handling stress preserved the structural integrity of the film, allowing for a complete and controlled release process over time.

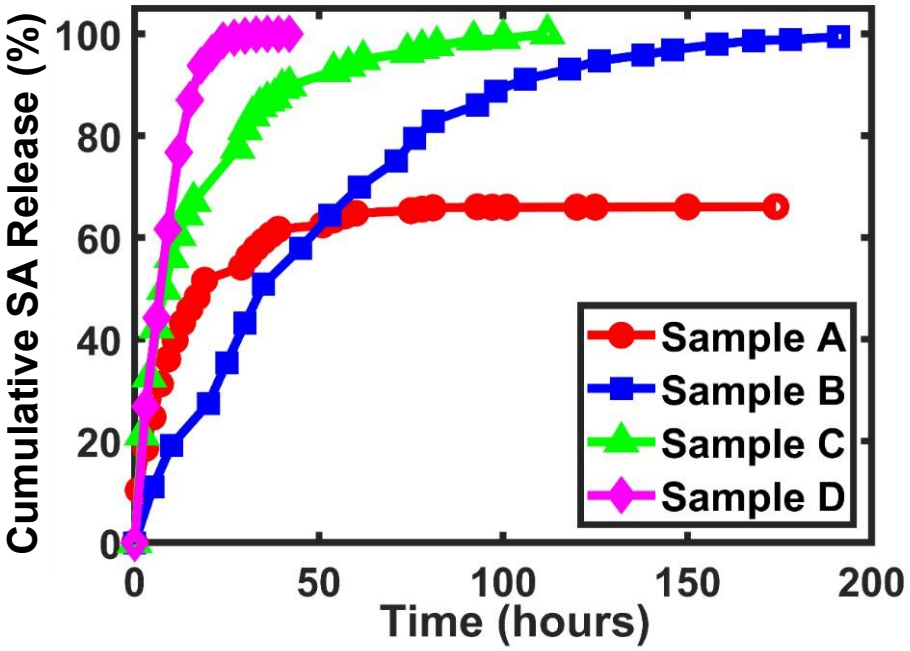

Figure 5: Cumulative SA release profiles of samples A, B, C and D over time.

In contrast, sample C exhibited comparatively faster SA release, reaching 100% within 112 hr. This rapid release behavior suggests that sample C had a more open polymeric network, likely due to crosslinking differences or increased polymer swelling, which facilitated faster SA diffusion compared to samples A and B. Sample D exhibited the most rapid SA release profile among all formulations, reaching 100% cumulative release within approximately 42 hr. This behavior contrasts with samples A and B, which showed more prolonged release, and even sample C, which completed release by 112 hr. The accelerated release in sample D can be attributed to the direct incorporation of SA into the PNIPAAM hydrogel matrix, potentially reducing SA polymer interactions and facilitating faster diffusion. Additionally, the presence of SA may have altered the hydrogel's internal microstructure, enhanced water uptake and swelling, thereby promoting rapid transport. The burst release observed in the early hours indicates that a substantial portion of the biomolecule was loosely bound or located near the surface of the polymer matrix, supporting the hypothesis of a highly permeable and less retentive network.

Comparative model fitting across the hydrogel formulations enabled identification of the dominant release mechanisms and assessment of how polymer composition and structure influence SA release kinetics (**Supporting Information C**). Samples A, B, and C showed strong agreement with the Korsmeyer–Peppas model, with the fitted n values indicating non-Fickian (anomalous) transport. This suggests that SA release was governed by a coupled mechanism of diffusion and polymer chain relaxation, rather than purely Fickian diffusion. In contrast, sample D exhibited a

different release profile. The Korsmeyer–Peppas model was not suitable for reliable fitting as more than 60% of total SA was released before the model's valid fitting window ended.

Based on the combined experimental release profiles and computational modeling results, sample B was selected for all subsequent experiments due to its superior sustained-release behavior, structural integrity, and near-complete SA release (99.5% at 191 hr).

3.2 Analysis of LCST and Swelling Properties of the Hydrogel

The visual transformation captures the thermoresponsive behavior of PNIPAAM hydrogels in aqueous media (Figure 6a). At temperatures below the LCST (~32 °C) [34,45], the hydrogel remains transparent or slightly translucent due to its hydrated, swollen state, where polymer chains form hydrogen bonds with water molecules. However, upon heating above the LCST, the polymer undergoes a reversible phase transition, becoming opaque and white in appearance (Figure 6a). This transition is driven by the collapse of the hydrogel network as hydrogen bonding with water is disrupted, leading to dehydration and aggregation of the polymer chains into a more compact, hydrophobic structure [34,45]. The resulting increase in light scattering accounts for the distinct white coloration observed in the upper portions of the test tubes. This optical change confirms the classic coil to globule transition of PNIPAAM in aqueous systems and is a hallmark of its temperature sensitive switching properties, critical for applications in drug delivery [34,45].

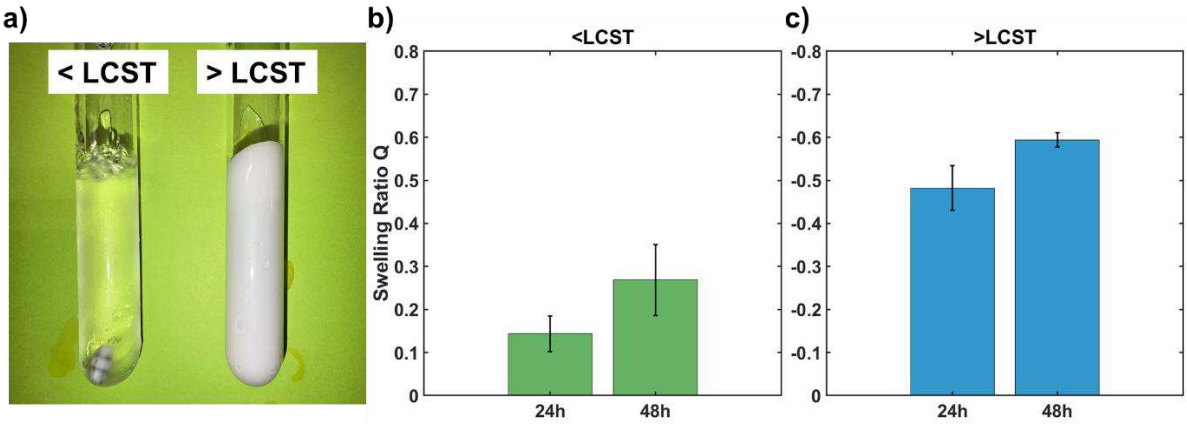

Figure 6: a) Visual representation of the phase transition behavior of PNIPAAM hydrogel across its LCST. The left test tube displays the hydrogel in its swollen, transparent state below LCST, while the right test tube shows the hydrogel in its collapsed, opaque state above LCST. b) Swelling behavior of pure PNIPAAM hydrogels below the LCST and c) deswelling behavior of pure PNIPAAM hydrogels above the LCST over 24 and 48 hr. Data are presented as mean ± standard deviation (n = 3 in each group).

Swelling and deswelling behaviors of PNIPAAM hydrogels were evaluated at three time points: initially (T = 0), after 24 hr, and after 48 hr. For the swelling experiments, hydrogels were submerged in 10 mL of deionized (DI) water at room temperature (23 °C), which is below the polymer's LCST. To assess deswelling, samples were submerged in 10 mL of DI water at a temperature above the LCST (>32 °C). At each time point (24 h and 48 h), hydrogels were gently removed from sealed containers and blotted lightly with absorbent tissue to remove surface water before weighing. The swelling ratio (Q) was calculated using the following equation [46–48]:

$$Q = \frac{W_t - W_o}{W_o} \quad (1)$$

Here,

W_o = the initial mass of the dry or reference sample at T = 0 hr.

W_t = The mass of swollen/shrunk sample at time T = 24 hr and T = 48 hr.

A positive Q value indicates water uptake (swelling), while a negative Q value indicates mass loss (deswelling). For example, Q = 1 corresponds to a doubling of the initial mass due to water absorption, whereas Q = −0.2 indicates a 20% reduction in mass. All experiments were conducted with three replicate hydrogel samples per condition [46–48]. As shown in Figure 6b, the swelling ratio (Q) under sub LCST conditions increased from 0.14 ± 0.04 in 24 hr to 0.27 ± 0.08 at 48 hr, indicating a gradual uptake of water over time. This behavior aligns with PNIPAAM's hydrophilic state below its LCST, where hydrogen bonding with water facilitates swelling [49,50]. In contrast, under super LCST conditions, where the polymer becomes hydrophobic, the hydrogels exhibited deswelling behavior. The Q value decreased from -0.48 ± 0.05 in 24 hr to -0.59 ± 0.02 at 48 hr, reflecting continued mass loss due to the temperature induced collapse of the hydrogel network. From 24 hr to 48 hr the hydrogel shrunk by 11% (Figure 6c). These negative Q values reflect water loss due to thermally induced hydrophobic collapse of the PNIPAAM network. The results confirm the characteristic temperature responsive behavior of PNIPAAM, with a clear distinction between its swelling and deswelling profiles driven by environmental temperature relative to its LCST [34]. Another experiment was done where the initial dry weight of the hydrogel was 219.1 mg, and after 3 days of immersion in PBS (pH = 7.4), the weight increased to 411.1 mg, resulting in a swelling ratio of 87.7%. This indicates that the hydrogel absorbed a significant amount of PBS, though it did not reach full hydration capacity. These findings are comparable to the PNIPAAM-co-AA (acrylic acid) hydrogels reported by Demirdirek and Uhrich [46], where the swelling behavior was influenced by pH and temperature, primarily due to the ionization of acrylic acid groups. However, since the PNIPAAM used in this study does not contain AA, its swelling ratio is expected to be lower than PNIPAAM-co-AA, which exhibits enhanced water uptake due to the presence of hydrophilic carboxyl groups. This suggests that while pure PNIPAAM swells effectively in PBS, it lacks the ionization driven swelling enhancement observed in acrylic acid containing hydrogel systems [47,48].

3.3 In Vivo Hormone Release in Grown Plants

3.3.1 Group 1

Group 1 contains three bell pepper plants labeled 1A, 1B, and 1C treated with SAPAE encapsulated hydrogel films upon showing stress (Table 1). The daily RH measurements are presented in Figure 7, while Figure 8a-c presents the visual condition of the plants post treatment on Day 10. On Day 1 (D1), the initial leaf RH readings were relatively high for all three plants (1A, 1B, 1C), particularly for plant 1C, which exhibited values in the 77% range (Figure 7), consistent with an unstressed, fully hydrated physiological state. Over the following days, as water was withheld and the plants were placed outdoors in direct sun to simulate drought like conditions, a steady decline in RH was observed across all plants. This reduction aligns with the expected

physiological response of stomatal closure, wherein the plant conserves water under stress, thereby reducing transpiration and local humidity near the leaf surface.

Plant 1A showed progressive RH declines from Day 1 to Day 5 (≈42% to 23%) (Figure 7). Hence, the SAPAE films were added to the root zone on Day 5. After 24 hr (Day 6), a notable increase in RH was detected, suggesting partial recovery of stomatal conductance and transpiration in response to SA release from SAPAE. Continued daily watering with small volumes of warm water (above PNIPAAM's LCST) targeted near the film site allowed for ongoing release, and by Day 8, RH levels gradually increased. By Day 9–10, a significant rise in RH was recorded (approaching or exceeding 50%), accompanied by visual improvement in leaf structure and turgidity, indicating a positive physiological recovery (Figure 8a).

Plant 1B showed almost a flat trend from Day 1 to Day 5 and a significant drop in RH on Day 6 likely due to water stress and direct sunlight. Following hormone application, a sharp increase in RH was observed on Day 7, which remained stable through Day 9. On Day 10, RH rose again by approximately 9%, indicating the plant's progression toward recovery, an observation further supported by its visible physical improvement (Figure 8b). Plant 1B's delayed response may be attributed to several possible factors such as slower root uptake kinetics, reduced film soil contact or uneven wetting, which could have delayed SA release or uptake, or individual plant variability in stomatal sensitivity or SA signaling.

By Day 6 (D6), plant 1C displayed a marked drop in RH to approximately 20%, indicating a sustained stress state. Visual signs of dehydration also became apparent, including fragile and brittle leaves, which are typical consequences of cellular turgor loss under prolonged water deficit. Based on this significant decline, SAPAE films were introduced into the soil via a 2 mL vial, and around it 15 mL of warm water (above PNIPAAM's LCST) was applied to initiate controlled release of SA. After 24 hr (Day 7) of the application of SAPAE, a notable increase in RH was detected in plant 1C, suggesting partial recovery of stomatal conductance and transpiration in response to SA release from SAPAE. Continued daily watering with small volumes of warm water targeted near the film site allowed for ongoing release, and by Day 8-9, RH levels were same. By Day 10, the RH was recorded at around 55%, accompanied by visual improvement (Figure 8c).

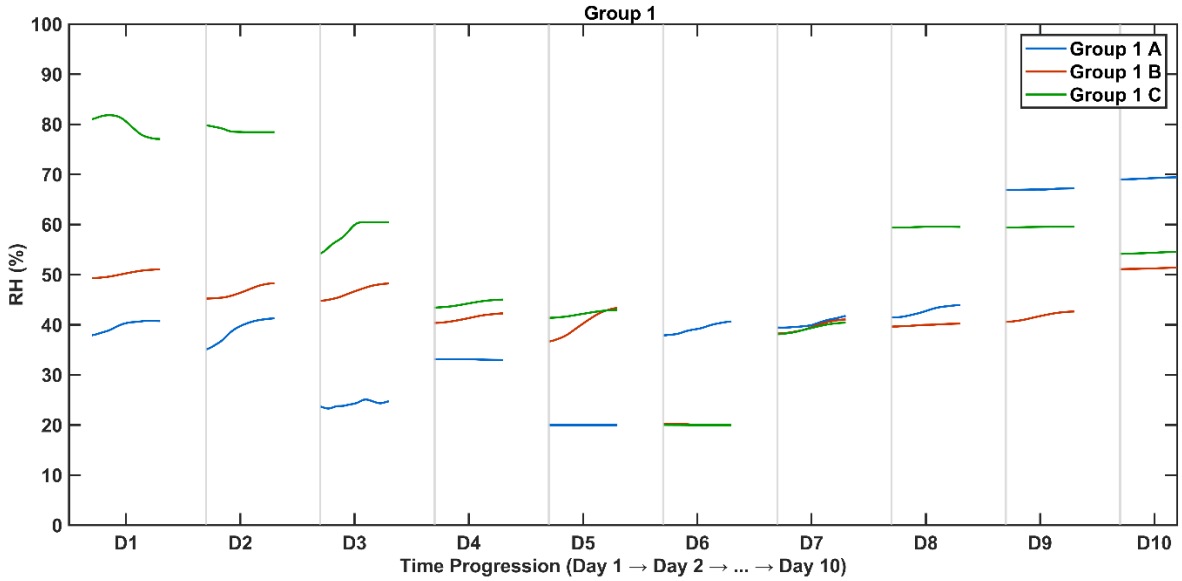

Figure 7: Daily leaf RH measurements for Group 1 bell pepper plants (1A, 1B, 1C) over a 10-day period. Each line represents an individual plant's humidity trend, captured daily over 20-minute intervals using sensors mounted on the abaxial leaf surface. SAPAE films were introduced on Day 5 for 1A and Day 6 for 1B and 1C, followed by warm water to trigger SA release.

All three plants show visibly improved morphology (Figure 8a-c) following SAPAE film treatment and gradual recovery from drought induced stress. Increased leaf turgor, upright posture, and overall plant vitality correspond with the elevated leaf surface RH values recorded after treatment, suggesting effective hormonal response and improved transpiration activity. Plant 1C exhibited the longest vertical root of ~192 mm (Figure 8f), while plant 1B showed the widest spread of ~83 mm (Figure 8e). Root dimensions are presented for qualitative assessment only, as growth within constrained plastic containers may have affected the natural direction and morphology of root development. Measurements reflect general health but are not definitive indicators of treatment efficacy.

Most stomata appear partially or fully open as shown in the SEM images (Figure 8g-h), suggesting a post recovery state following SAPAE application. Quantitative assessment of stomatal aperture in SAPAE treated Group 1 plants revealed a mean opening length of 1.932 µm, with a standard deviation of ±0.949 µm, indicating moderate variability in stomatal responsiveness. The maximum measured aperture was 3.289 µm, while the minimum was 0.407 µm (Table D.1, Supporting Information). These results suggest that the stimulus responsive delivery of SA facilitated partial to substantial reopening of stomata under drought conditions. This quantitative finding supports both the SEM based qualitative observations and the RH sensor data, confirming physiological recovery at the leaf surface level.

These findings suggest that SAPAE triggered SA delivery supported partial restoration of stomatal opening, enabling the resumption of transpiration and indicating improved plant water status. The results from Group 1 reinforce the linkage between localized RH at the abaxial leaf surface, stomatal dynamics, and plant stress physiology. During drought conditions, RH declines due to stomatal closure and reduced transpiration. In contrast, the recovery of RH following SAPAE administration suggests reopening of the stomata, potentially induced by SA-mediated

activation of stress tolerance mechanisms known to enhance plant resilience under water-deficit conditions. This shows the potential of SAPAE films to modulate plant response in real time via environmentally triggered, root mediated hormone uptake.

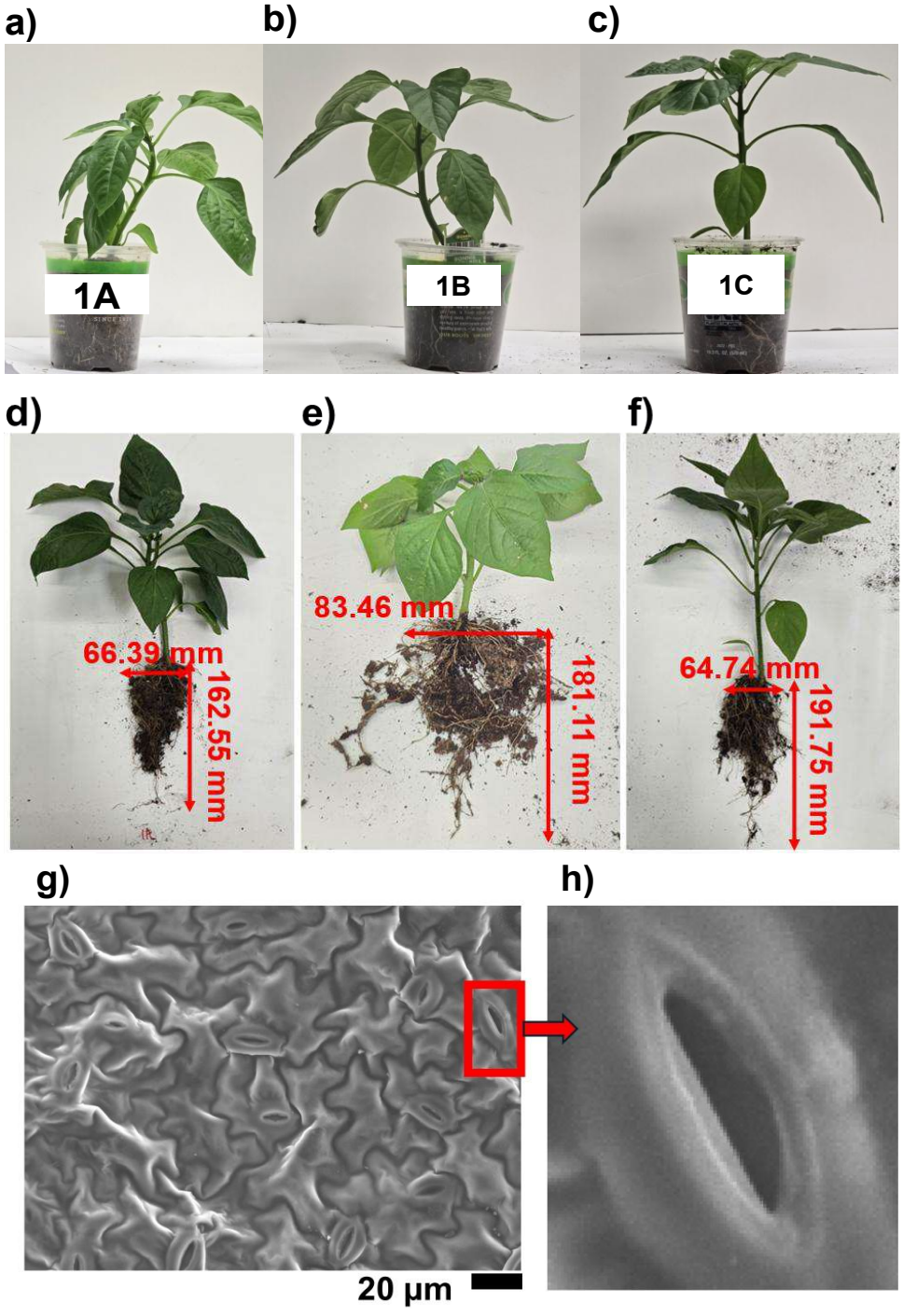

Figure 8: Post treatment photographs of Group 1 bell pepper plants on Day 10: a)-c) full canopy view and d)-f) root architecture view. The red annotations represent horizontal root spread and vertical root length. g) High resolution SEM image (scale bar: 20 µm) of the abaxial leaf surface from Group 1 plants on Day 10. h) A representative stomatal aperture is shown magnified on the right.

3.3.2 Group 2

In Group 2, three bell pepper plants (labeled 2A, 2B, and 2C) were monitored to investigate their physiological response to free SA delivered via film after the onset of drought stress. As illustrated in Figure 9, Plant 2A showed a decreasing trend in RH from approximately 45% on Day 1 to about 37.5% by Day 5, indicating a stomatal closure response to water stress. On Day 5, an SA film was introduced at the root zone with warm water to initiate release. A sharp rise in RH was observed on Day 6, suggesting a temporary reopening of stomata and increased transpiration. Over subsequent days, RH stabilized at ~65% by Day 10. This correlates well with the plant's physical appearance (Figure 10a), which showed relatively healthy leaf posture and turgor, suggesting partial recovery from drought stress likely supported by the SA treatment.

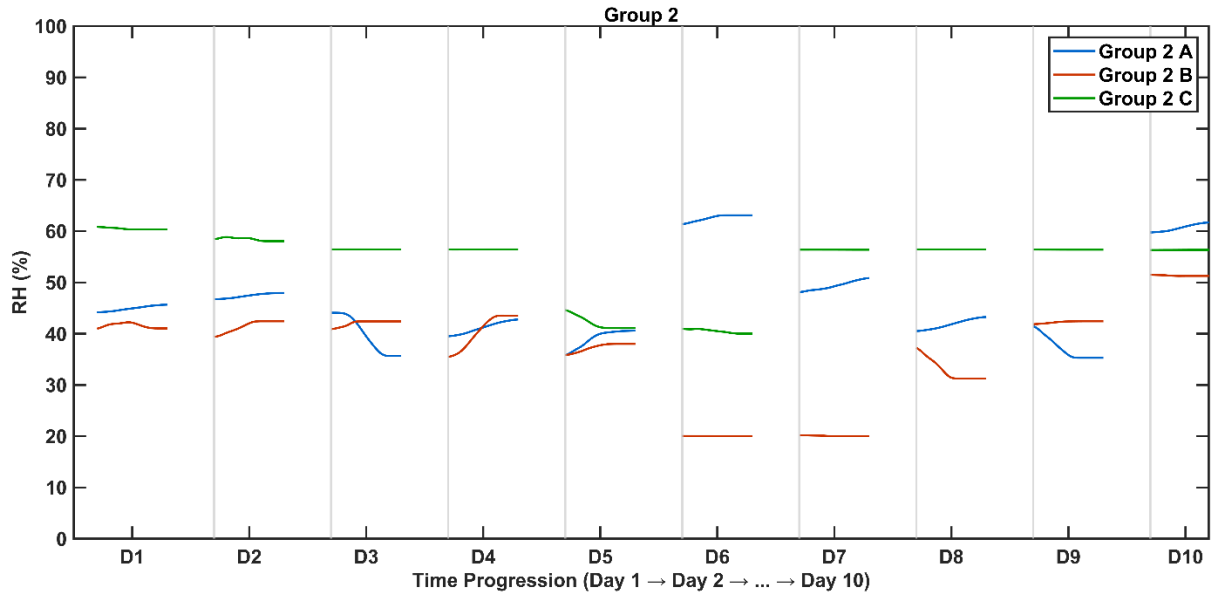

Figure 9: Daily leaf RH measurements for Group 2 bell pepper plants (2A, 2B, 2C) over a 10-day period. SA films were administered on Day 5 for 2A and on Day 6 for 2B and 2C.

In contrast, plant 2B was treated on Day 6 when its RH had dropped significantly. After SA film application, RH initially remained unchanged on Day 7 but then gradually increased to ~50% by Day 10. However, plant 2B maintained a wilted and stressed morphology, implying that the SA response may have been suboptimal or delayed in this specific plant (Figure 10b). This variation could be due to physiological differences such as root uptake rate, developmental stage, or heightened sensitivity to SA induced feedback regulation [51–53].

Plant 2C showed stable RH until Day 4 (~57.5%), followed by a decline around Days 5–6, coinciding with stomatal restriction. The SA film was applied on Day 6, resulting in a sharp RH increase on Day 7 (~57%), which remained relatively stable through Day 10. The plant maintained an upright leaf structure and overall healthy appearance, suggesting a positive recovery trajectory similar to 2A (Figure 10c).

Visual differences across the plants reflect varied physiological responses to SA film treatment (Figure 10a-c). Plant 2A and 2C appear relatively healthy with firm leaf posture, while

2B remains visually stressed, despite similar humidity measurements, suggesting potential inconsistency in hormonal uptake or response.

Plant 2A exhibited the longest vertical root (~202 mm) and widest spread (~91 mm), while 2C and 2B showed slightly reduced dimensions (Figure 10d-f). Variations in root architecture likely reflect pre-existing differences in plant maturity, as the plants were commercially sourced and not grown under controlled conditions.

The SEM images of the abaxial surface of leaves reveal several partially open stomata, though the aperture sizes vary across the field of view (Figure 10g-h). This partial opening may suggest inconsistent stomatal regulation following free SA application, consistent with the variable RH data and mixed recovery patterns observed in Group 2. Stomatal aperture analysis in Group 2 plants showed a mean opening length of 1.581 µm with a standard deviation of ±0.871 µm (Table D.1, Supporting Information). The aperture range extended from 0.547 µm to 2.751 µm, indicating moderate variability and generally narrower openings compared to SAPAE treated plants. The lower mean aperture and limited maximum opening further support the conclusion that free SA film (Group 2) was less effective in consistently reversing stomatal closure than SAPAE-loaded films (Group 1).

Together, the results from Group 2 indicate that free SA application can support recovery from drought stress, evidenced by increased RH and improved visual health. However, the kinetics of SA release and the plant's physiological response appear more variable than those observed in the SAPAE treated Group 1. A likely explanation is that free SA may exhibit burst release behavior, potentially leading to transient hormonal overexposure and inconsistent stomatal regulation. While SA is recognized for improving drought tolerance, excessive or improperly timed application can trigger oxidative stress or disrupt normal hormonal signaling, potentially contributing to the varied response observed in plant 2B. Additionally, while plant 2C maintained relatively high RH and general vigor, slight wilting of the leaves was observed, alongside the presence of a developing flower bud (Figure 10c). This suggests that the plant may have entered a reproductive phase, which often alters hormonal balance and resource allocation, potentially explaining the subtle signs of water stress despite stable humidity readings. During flowering, plants frequently redirect energy from vegetative maintenance to reproductive structures, which can transiently reduce turgor or delay full recovery under stress [54]. These observations reinforce that while SA has a known regulatory role in mitigating abiotic stress, the method of delivery (sustained vs. burst) and plant specific sensitivity must be carefully considered for consistent stress adaptation in crop systems.

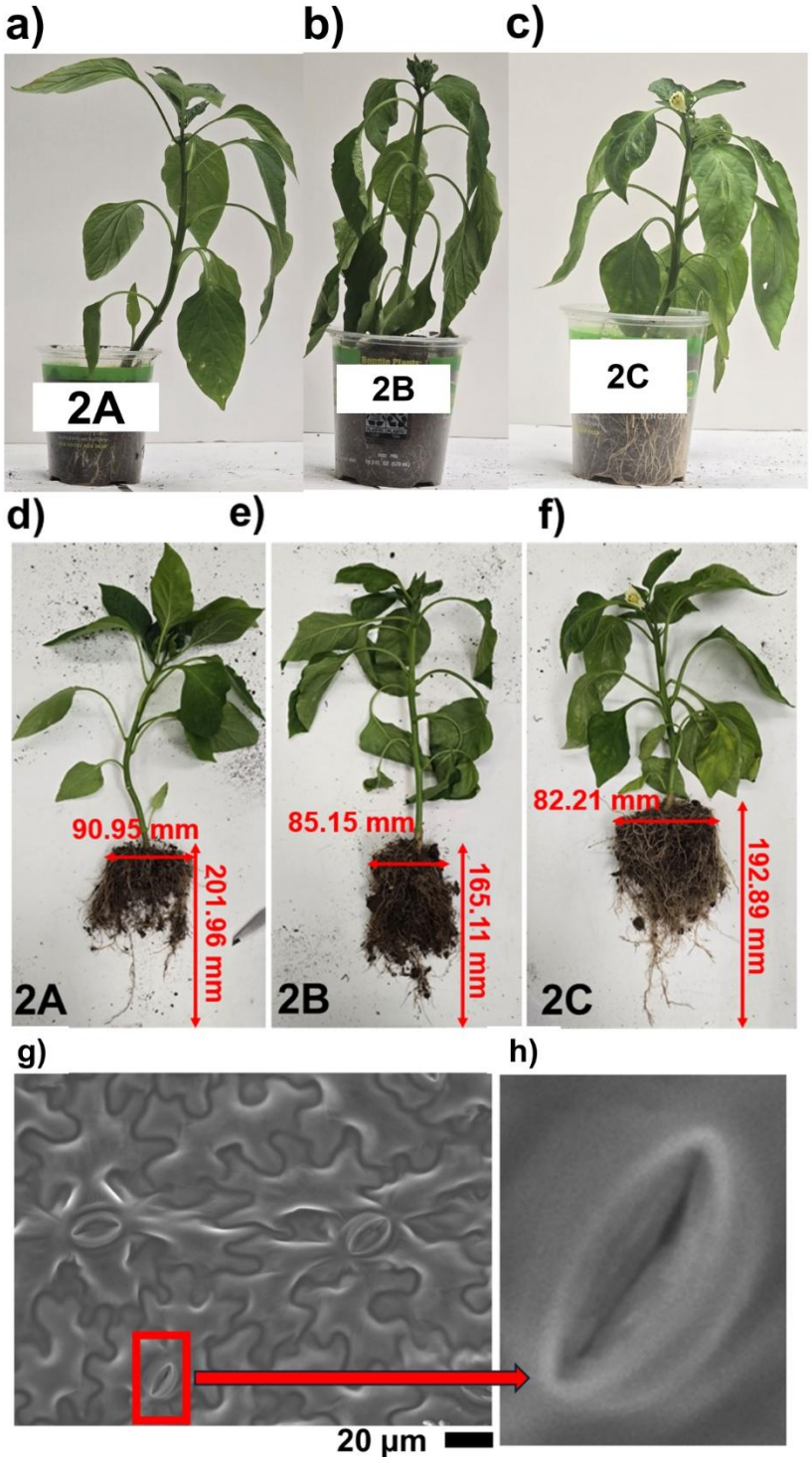

549

550 **Figure 10: Post treatment photographs of Group 2 bell pepper plants on Day 10: a)-c) full canopy view and d)-**
551 **f) root architecture view. The red annotations represent horizontal root spread and vertical root length. g) High**
552 **resolution SEM image (scale bar: 20 µm) of the abaxial leaf surface from Group 2 plants on Day 10. h) A**
553 **representative stomatal aperture is shown magnified on the right.**

554

3.3.3 Group 3

Group 3 served as the drought stressed, untreated group, wherein the three bell pepper plants (labeled 3A, 3B, and 3C) were subjected to the same stress protocol as other groups but received no external hormone films or irrigation after the initial acclimation period (Figure 11). The aim was to establish a baseline of unmitigated drought progression in the absence of hormonal intervention.

Plants 3A and 3C exhibited a progressive decline in leaf surface RH over the 10-day period, with RH values dropping below ~20% by Day 10. This decline is consistent with severe stomatal closure, a well-documented drought response wherein the plant reduces water loss via transpiration under stress. However, prolonged stomatal closure can lead to impaired gas exchange, metabolic suppression, and ultimately cellular damage. Correspondingly, pronounced wilting, leaf droop, and general loss of turgor were observed in plants 3A and 3C (Figure 12a, c), thus indicating advanced physiological stress and possible irreversible damage.

Plant 3B initially followed a decreasing trend, but around Day 7, RH values began to increase moderately and continued to rise and then decreased on Day 10, reaching ~32.5% (Figure 11). While no external hormone or water was applied, the RH increase on Day 7 may be attributed to the plant's relocation from high heat outdoor conditions to the relatively cooler laboratory environment. The transfer was necessary due to visible signs of severe heat stress, such as wilting and leaf desiccation, indicating a risk of irreversible physiological damage if exposure to high temperatures continued. Reduced VPD in the lab may have facilitated passive water retention, leading to a transient rise in RH near the leaf surface [55]. Nonetheless, Figure 12b shows that plant 3B remained visually wilted, and the recovery was not sufficient to restore leaf structure or vitality.

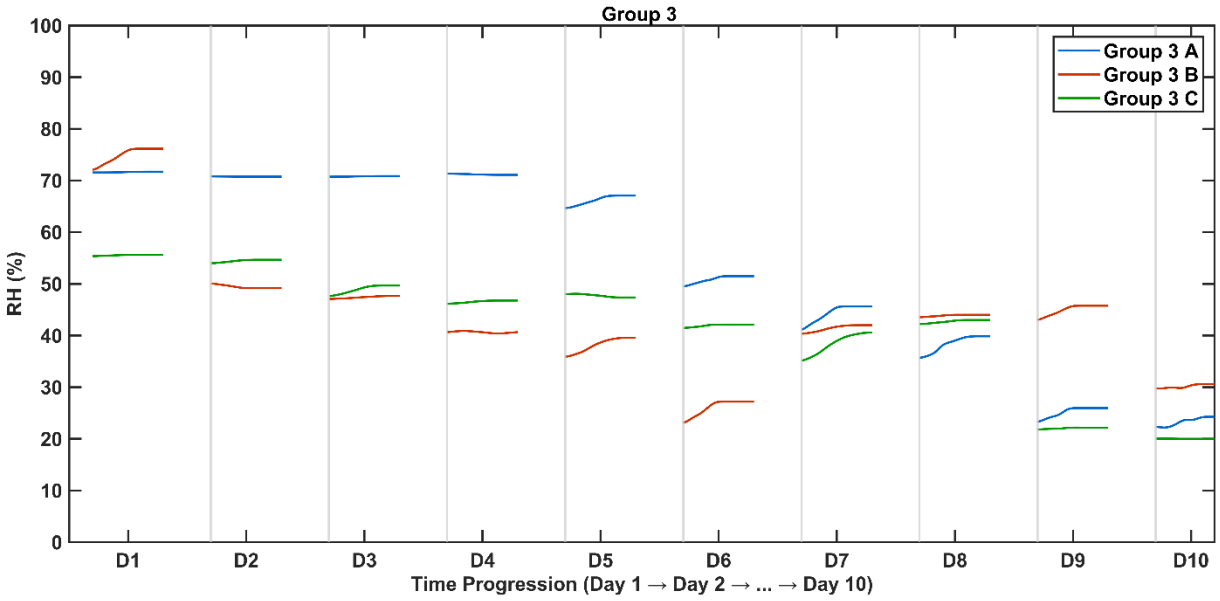

Figure 11: Daily leaf RH measurements for Group 3 bell pepper plants (3A, 3B, 3C) over a 10-day period. No hormone treatment was applied throughout the experimental period.

All three plants exhibited reduced leaf turgor and signs of severe stress (Figure 12a-c). Root systems, while still measurable, appeared thinner and less fibrous compared to SA treated groups (Figure 12d-f).

Figure 12g-h reveals primarily closed stomata or severely constricted apertures, consistent with sustained water stress and stomatal suppression. Stomatal aperture measurements in Group 3 demonstrated a mean opening of only 0.396 µm, with a narrow standard deviation of ±0.138 µm, and a maximum aperture of only 0.538 µm (Table D.1, Supporting Information). These values reflect a significantly restricted stomatal state, indicative of strong stomatal closure under prolonged water deficit. The narrow aperture range also suggests limited variability in stomatal responsiveness across the field. These quantitative findings align with qualitative SEM observations, low RH sensor data, and the visibly wilted phenotype, confirming a sustained stress state and suppressed transpiration capacity in the absence of SA mediated recovery.

Overall, these findings emphasize the essential role of external interventions, such as hormonal stimulation or rehydration, in facilitating plant recovery under severe abiotic stress conditions. Without intervention, drought induced stomatal closure and suppressed transpiration led to a sustained decline in RH, culminating in plant deterioration. The differing results between Groups 1-2 and 3 underscore the therapeutic benefits of SA delivery under drought conditions. Thus, Group 3 strongly suggests that natural recovery is not achievable under continuous water limitations, even when environmental severity is reduced, and that external stimuli is essential for reversing the physiological trajectory under drought conditions.

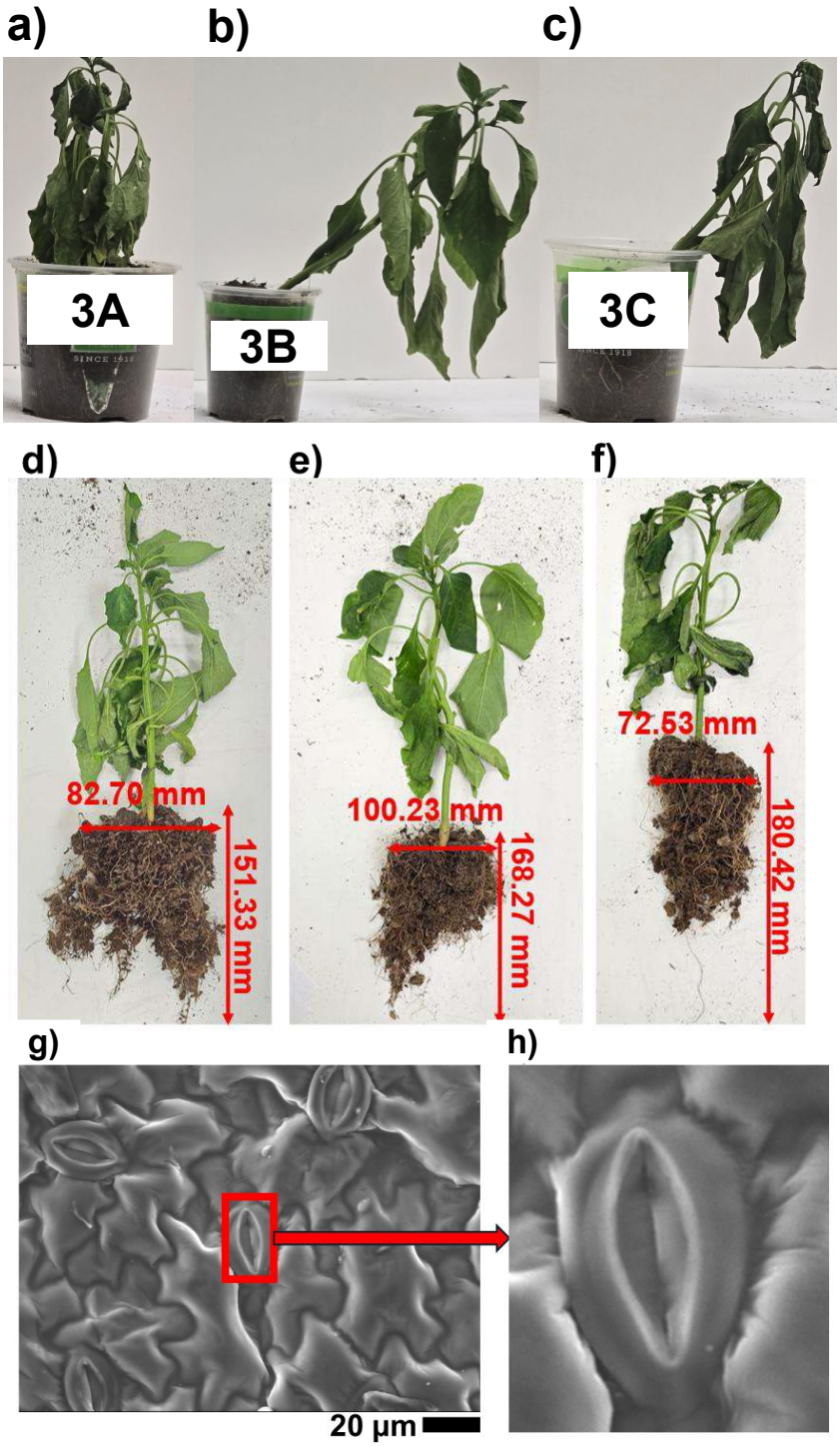

602

603 **Figure 12: Photographs of Group 3 bell pepper plants on Day 10: a)-c) full canopy view and d)-f) root**
604 **architecture view. The red annotations represent horizontal root spread and vertical root length. g) High**
605 **resolution SEM image (scale bar: 20 µm) of the abaxial leaf surface from Group 3 plants on Day 10. h) A**
606 **representative stomatal aperture is shown magnified on the right.**

607

3.3.4 Group 4

For Group 4 (the true control group), the plants were watered daily and placed in an area with moderate sunlight exposure to maintain normal growing conditions and avoid drought induced stress. All the three plants (4A, 4B and 4C) showed an almost higher RH than the other groups (Figure 13). These plants also showed a healthy physical appearance after 10 days (Figure 14a-c).

Notably, plants 4A and 4C maintained RH levels between ~50% and 65% beyond Day 4, with minimal fluctuations, reflecting stable water status and unrestricted gas exchange, which are hallmarks of a non-stressed physiological state. The RH variations observed are likely related to normal developmental processes, including leaf expansion and diurnal variations in stomatal aperture, rather than external stress.

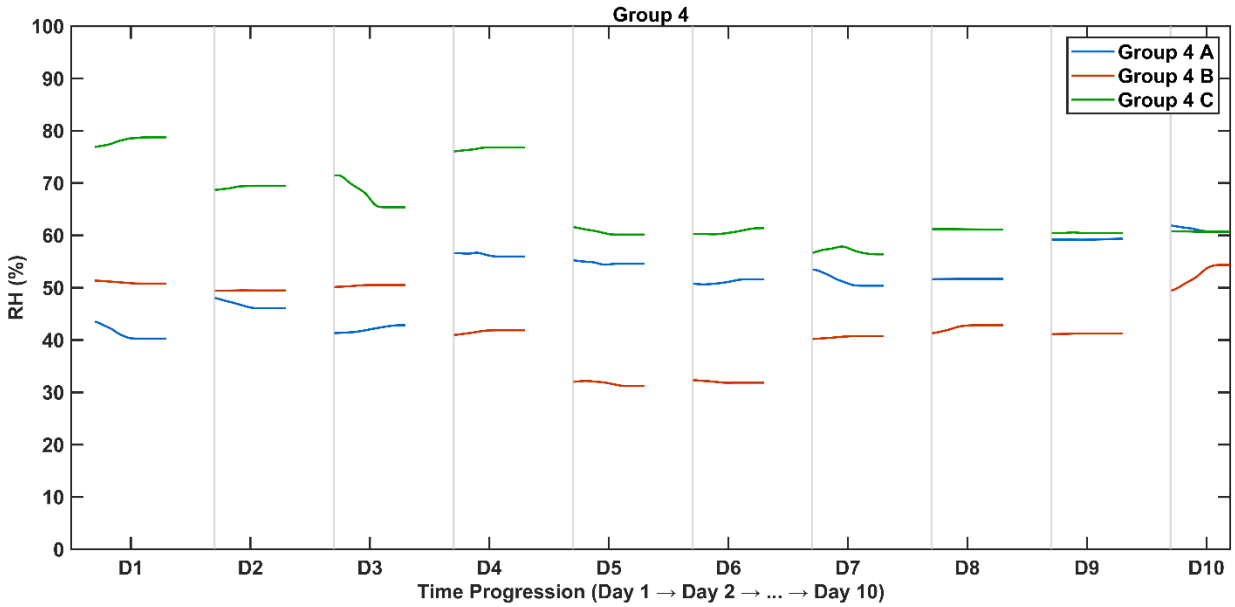

Figure 13: RH trends of Group 4 bell pepper plants (4A, 4B, 4C) under well-watered, non-stress conditions over a 10-day period. All three plants were maintained with regular irrigation and moderate sunlight exposure. Stable RH levels indicate consistent transpiration activity and stomatal function. Slight variability in plant 4B may reflect internal redistribution of water due to active fruit development.

Plant 4B, however, exhibited slightly lower and more variable RH values, decreasing from approximately 50% on Day 1 to around 30% by Days 5–6. Upon phenotypic inspection (Figure 14b), this plant was found to be in an active fruiting stage, with a visible developing pepper. Two flower buds were also observed on Day 1 but had senesced by mid experiment, leaving only the fruit in development. The onset and progression of fruit development are known to divert internal water and energy resources and can influence stomatal regulation and transpiration rates [56]. The relatively lower RH levels in this plant may therefore reflect a redistribution of water toward reproductive organs, temporarily altering local transpiration dynamics. Despite this, all three plants in Group 4 maintained healthy morphological traits, including firm leaf turgor, upright posture, and robust growth (Figure 14a-c).

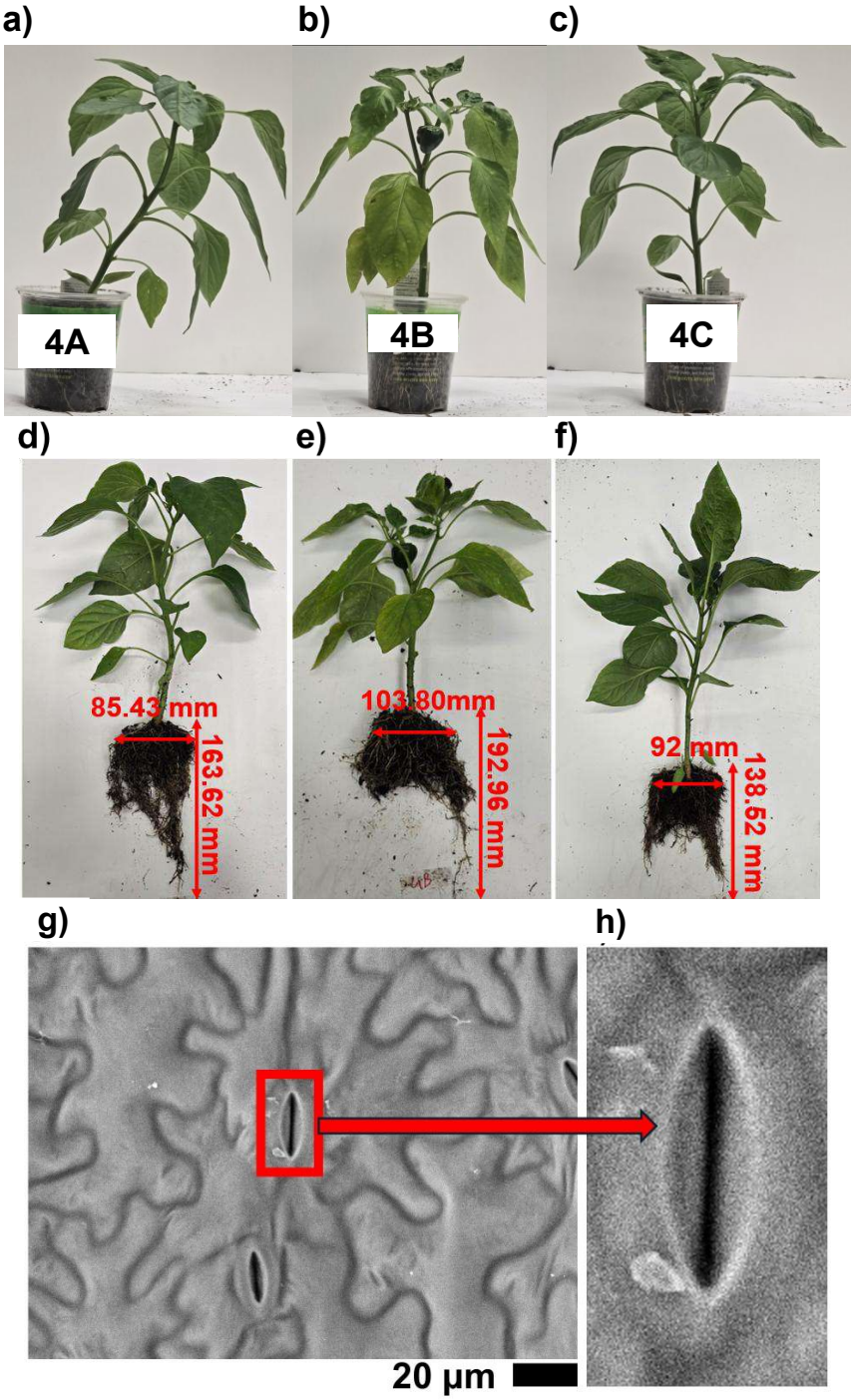

634

635 **Figure 14: Photographs of Group 4 bell pepper plants on Day 10: a)-c) full canopy view and d)-f) root**
636 **architecture view. The red annotations represent horizontal root spread and vertical root length. g) High**
637 **resolution SEM image (scale bar: 20 µm) of the abaxial leaf surface from Group 4 plants on Day 10. h) A**
638 **representative stomatal aperture is shown magnified on the right.**

639 Plant 4B exhibited the widest root spread (~104 mm), while vertical lengths ranged from
640 ~139 mm to ~193 mm depicting a baseline compared to other stressed groups (Figure 14d-f).

Numerous stomata appear open or partially open, consistent with the plants' healthy hydration status and uninhibited transpiration observed during the experimental period (Figure 14g-h). These images represent the most physiologically active stomatal states among all the four groups. The dense stomatal distribution and well-defined guard cell structures provide supportive evidence for active gas exchange in unstressed plants. The mean stomatal opening length was 2.041 µm, with a standard deviation of ±0.529 µm, and an aperture ranging from 1.077 µm to 3.857 µm (Table D.1, Supporting Information). This broad distribution reflects robust stomatal opening and high variability in aperture sizes consistent with normal physiological fluctuations under optimal hydration. The results align with RH sensor data and qualitative SEM images, indicating active transpiration and a healthy gas exchange profile.

The findings from this group validate that in the absence of external abiotic stress, bell pepper plants can sustain stable transpiration and physiological performance. The recorded RH and stomatal aperture data serve as a baseline for comparison against drought stressed and hormonally treated groups. A comparative summary of all groups is presented in **Supporting Information D**.

3.4 In Vivo Hormone Release in Seeds

3.4.1 Phase 1 with Tomato Seeds

On Day 1, tomato seeds were sown in each of the three pots, which were maintained under identical environmental conditions throughout the study (Figure 15a). No visible germination or morphological changes were observed in the seeds until Day 7. By Day 8 (Figure 15b), early signs of germination were observed in the pots containing the SAPAE film. A small, developing seedling was clearly visible in the SAPAE treated group, while a faint, underdeveloped shoot structure was also noted in the SA film treated pot. However, to preserve the experimental integrity and avoid disrupting the soil film interface or hydrogel triggered hormone release dynamics, the seedlings were not removed or disturbed at this intermediate stage.

The observation period was extended to 14 days to evaluate the sustained effects of hormone release under simulated drought conditions. By the end of the two-week period, only the seedlings grown with the SAPAE film exhibited continued development, displaying visibly elongated and healthy shoot structures (Figure 15c). This was further confirmed by retrieving fully sprouted seedlings from the SAPAE-treated pots after 14 days and imaging them under an optical microscope (Leica M205A Encoded Stereo Microscope, Leica Microsystems, Germany). The microscopic images reveal a pronounced elongation of the hypocotyl and early leaf formation on Day 14 compared to Day 1 (Figure 15d-e). In contrast, no viable seedling was present in the SA treated pot (Figure 15c). This suggests that the initially visible shoot may have undergone senescence or failed to progress, potentially due to a high concentration burst release of free SA, which is known to exhibit phytotoxic effects at elevated levels [57]. The sustained presence and enhanced growth of the seedling in the SAPAE treated group highlights the advantage of biomolecule-based delivery systems for gradual and localized hormone release. SAPAE's hydrolysis driven release mechanism allowed for controlled, prolonged exposure to SA, thereby promoting seedling survival and drought tolerance without overwhelming the plant tissue. These findings underscore the significance of dosage kinetics and hormone delivery strategy in modulating plant stress responses and developmental outcomes.

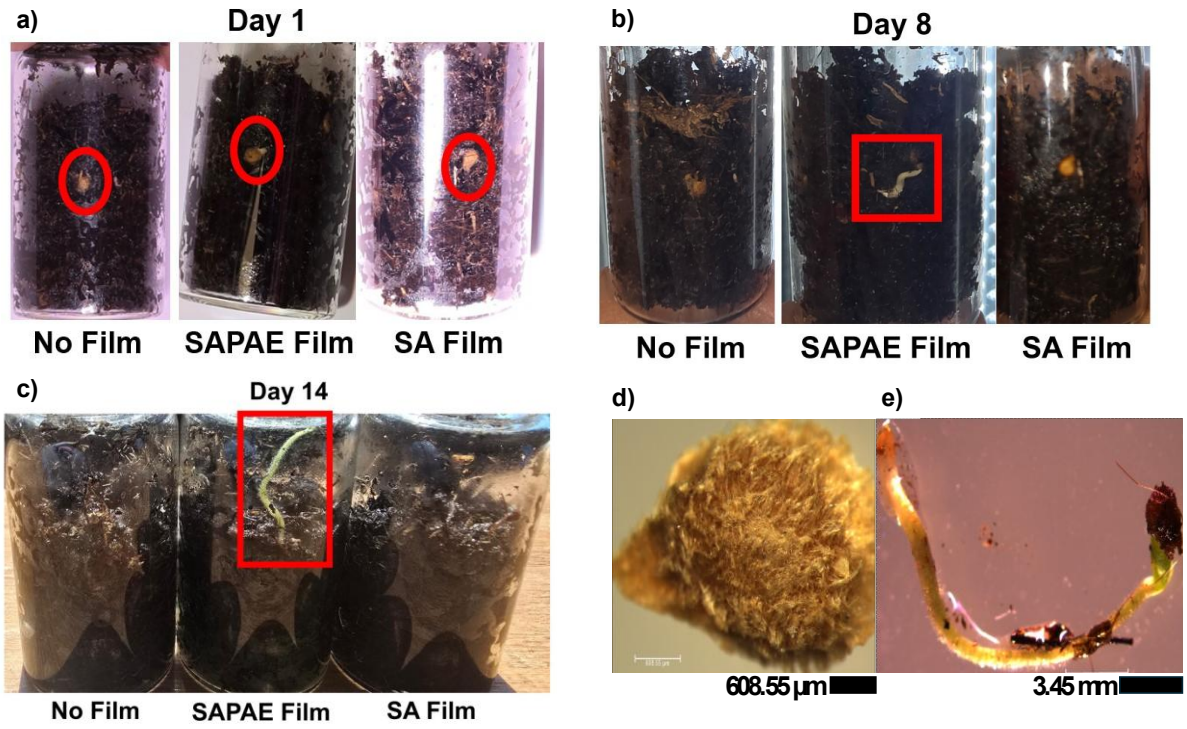

Figure 15: a) Initial condition of tomato seeds placed in three different pots on Day 1: (left) no film, (middle) SAPAE loaded film, and (right) free SA film. Red circles highlight the seeds. b) Seed germination progress observed on Day 8 under drought mimicking conditions in the same treatment groups. A clear emergence of seedling is visible in the SAPAE group (highlighted with a red box). c) Seedling development observed on Day 14 across the three treatment groups. A prominent seedling emergence with visible hypocotyl elongation is observed in the SAPAE treated pot (highlighted in red). d) and e) Optical microscopic images of tomato seed development under SAPAE treatment: d) Unaltered seed observed on Day 1 prior to sowing, with intact seed coat and trichome like surface features; e) Fully sprouted seedling on Day 14, showing elongated hypocotyl and early leaf formation.

3.4.2 Phase 2 with Bell Pepper Seeds

During the bell pepper seedling phase (Figure 16a), a distinct sprout was observed on Day 11 in Group 1 (Figure 16b), which received the SAPAE film treatment. This seedling was the only new emergence recorded across all experimental groups at that time. The sprout appeared healthy with visible hypocotyl and cotyledon structure, suggesting initial support from the SAPAE mediated SA release. However, by Day 14, the seedling was no longer visible or upright, indicating a subsequent failure in sustained development. The decline could be attributed to multiple interacting factors, including nutrient or water limitations, or the cumulative impact of prolonged drought stress. This pattern of early emergence followed by senescence reflects the sensitivity of early seedlings to fine balances in hormone release, water availability, and mechanical environment. These findings emphasize the need for precise optimization of hormone release profiles and environmental control when evaluating hormone loaded polymeric systems under complex abiotic conditions. This observation supports the previous trend noted in the tomato seed experiment, where early sprouting also occurred in SAPAE treated pots. However, unlike the earlier tomato study which was conducted inside a controlled artificial environmental chamber this

bell pepper experiment was performed in a standard laboratory setting. While the pots were maintained at approximately 35 °C using a water bath technique, the ambient air temperature remained at ~23 °C, introducing a thermal gradient that may have affected overall film responsiveness and internal pot conditions. Such environmental inconsistencies could interfere with the temperature dependent swelling deswelling behavior of PNIPAAM, potentially affecting the timing and extent of SA release from SAPAE films. Furthermore, species specific sensitivity may also play a critical role. Bell pepper seeds are known to exhibit stricter germination requirements and may be more susceptible to fluctuating environmental conditions compared to tomato seeds [58]. Variations in seed coat permeability, hormone sensitivity, and water uptake kinetics across species can significantly alter how seeds respond to the same treatment strategy.

Despite these challenges, it is noteworthy that both instances of early germination in this study occurred in SAPAE treated pots, reinforcing the effectiveness of sustained hormone delivery over burst applications. However, the subsequent decline of seedlings suggests that while SAPAE promotes early-stage activation, long term seedling survival is highly dependent on consistent environmental support and possibly tailored dosing for specific plant types. These findings highlight the need for seed specific optimization in hormone delivery systems and underscore the influence of environmental parameters especially temperature uniformity on polymer based smart release mechanisms.

The results from both tomato and bell pepper seed experiments suggest that SAPAE loaded hydrogel films have the potential to support early germination under drought-like conditions through the sustained and thermoresponsive release of SA. In both phases, initial sprouting was observed specifically in SAPAE treated pots, indicating a favorable effect of localized, controlled hormone delivery. However, despite early germination success, the continued survival of seedlings was not consistent particularly in the bell pepper study. Differences in experimental conditions, namely the use of an artificial environmental chamber in the tomato phase versus a standard laboratory setting in the bell pepper phase, as well as species specific physiological thresholds, may have contributed to these variations. These results underscore the importance of optimizing environmental stability, hormone concentration, and release timing for different seed types and stress contexts.

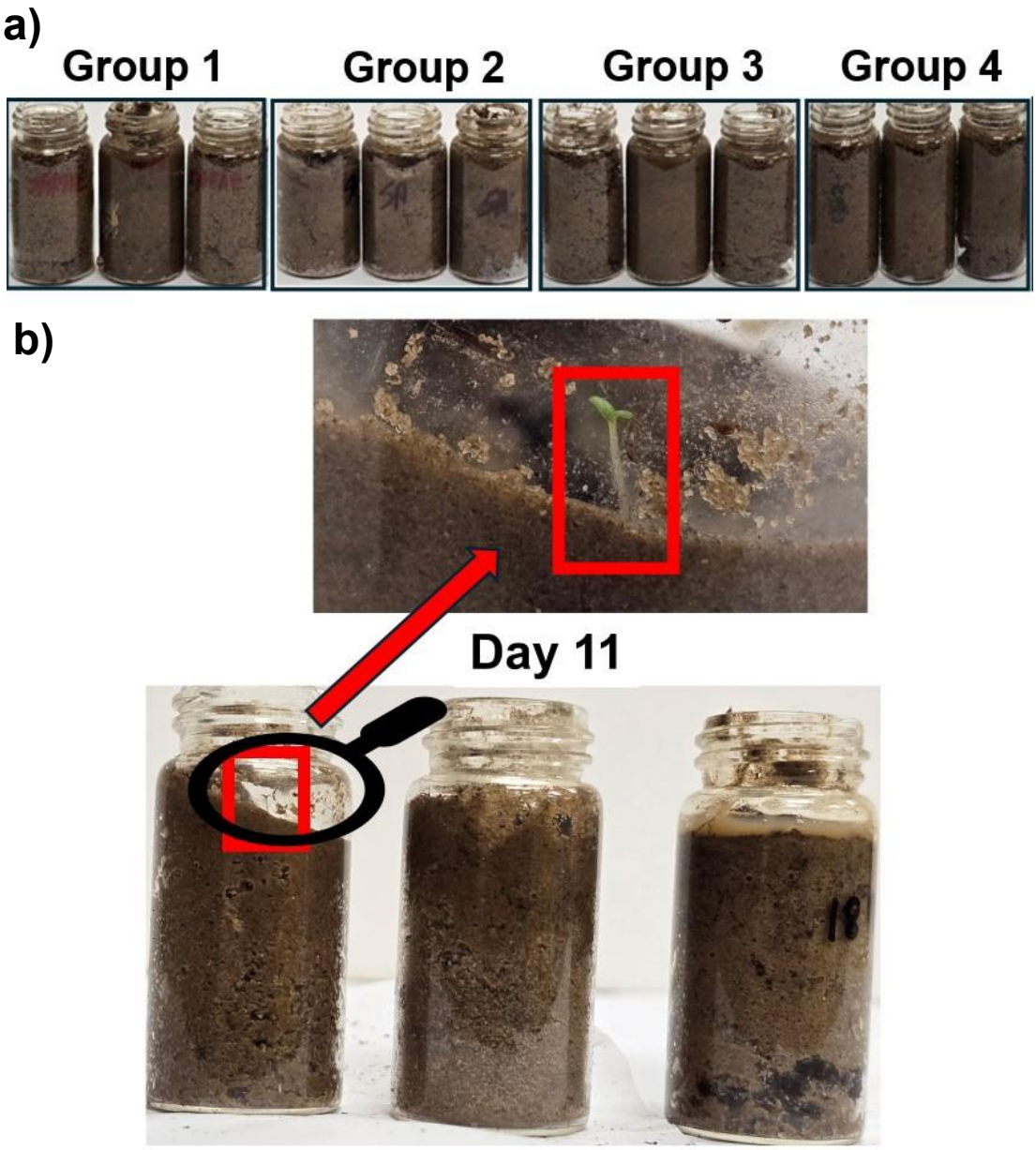

739

740 **Figure 16: a) Visual documentation of experimental setup on Day 1 for all four treatment groups in the bell**
741 **pepper seedling study. Each group consists of three pots, with seeds placed beneath films containing different**
742 **treatments. b) Emergence of a bell pepper seedling in Group 1 (SAPAE film treated). The lower panel shows**
743 **the three replicate pots on Day 11, with the leftmost pot exhibiting a visible sprout (highlighted and magnified**
744 **in the upper panel). This seedling was the only new emergence observed across all groups on Day 11.**

745

3.5 Performance Comparison

The comparative analysis presented in Table 3 evaluates different controlled release systems for SA and other plant hormones, highlighting their application method, materials used, and agricultural benefits. Traditional foliar spray and seed priming methods [59], [60] are effective for short term plant stress mitigation, but they lack sustained release, requiring frequent reapplications. Similarly, soil application techniques [61] contribute to ion homeostasis and root function improvement, yet rely on direct uptake by roots, which can be inconsistent under varying environmental conditions. The use of encapsulation techniques and hydrogel based controlled release systems [62], [63] has emerged as a promising alternative to traditional delivery methods. For instance, chitosan based salicylic acid nanocomposites (CS-SA-NCs) [62] demonstrate gradual SA release, improving salinity tolerance and antioxidant activity in grapevines. However, the exact release duration remains unspecified, limiting precise control over hormone availability. Encapsulation of SA in silica and chitosan carriers [63] has been shown to enable controlled release while minimizing adverse effects, with measurable plant responses observed for up to 12 days; however, the long-term release kinetics remain unclear. Similarly, hydrogel-based delivery systems [64] exhibit degradation-controlled release, with glycoalkaloid bioactive compounds released for up to 21 days in aqueous environments, suggesting a potentially longer though not yet fully quantified release duration in soil.

While these systems extend hormone availability, they rely on passive degradation mechanisms that lack responsiveness to changing environmental conditions and plant needs. This highlights the need for on-demand, plant-specific hormone delivery. In contrast, the present work introduces a thermo-responsive PNIPAAM hydrogel platform that enables stimuli-responsive release of SA, overcoming the limitations of passive systems. Importantly, hormone release is triggered based on real-time plant stress signals, specifically declines in leaf RH at the individual plant level. This closed-loop approach enables tunable release kinetics and adaptive, need-based hormone delivery, thereby improving the precision, reliability, and effectiveness of plant stress mitigation.

785 **Table 3: A comparative assessment of this study against existing literature on exogenous hormone application.**

Ref.	Application Method	Material	Agricultural benefits	Release Duration
[59]	Foliar spray on leaves	Water based SA solution	Improved tolerance to salinity stress, enhanced chlorophyll content, and increased yield attributes	-
[65]	Seed priming and foliar spray	SA + Thiourea in aqueous solution	Increased grain yield, improved relative water content, reduced lipid peroxidation under salinity and drought stress	-
[60]	Foliar spray on leaves	Water based SA solution	Improved photosynthetic efficiency, stomatal conductivity, and oxidative stress regulation under stress conditions	-
[61]	Soil application (Direct uptake via roots)	Water based SA solution	Enhanced ion homeostasis (Na^+/K^+ balance), improved root function under salinity stress	-
[62]	Foliar spray	Chitosan based SA nanocomposite (CS-SA-NCs)	Enhanced salinity tolerance, antioxidant activity, and photosynthetic efficiency	Not explicitly stated (gradual effects observed over study period)
[63]	Hydroponic medium	Silica nanoparticles (Si) + Chitosan (Ch) forming a composite encapsulating SA	Enhanced abiotic stress tolerance, maintenance of hormonal homeostasis	8–12 days of observance
[66]	Foliar spray and soil drench	Aqueous solution of abscisic acid (ABA) and indole-3-acetic acid (IAA) dissolved in water	Improved physiological and hormonal adaptation under long term waterlogging conditions	-
[64]	Hydrogel based controlled release	Alginate Ca^{2+} hydrogel or Carboxymethylcellulose Fe^{3+} hydrogel encapsulating Glycoalkaloid extracts from tomato and potato leaves	Reduced bacterial and fungal load, potential pesticide alternative	Up to 21 days in water (potentially longer in soil)
This work	**Hydrogel films put into soil**	**PNIPAAM hydrogel encapsulates SA for thermo-responsive release**	**Sustained delivery of SA for plant stress resilience, enhanced adaptability to environmental conditions**	**Experimentally shown for up to 8 days but can be tuned (days to weeks depending on stimulus response)**

786

4. Conclusion and Future Direction

This study presents an integrated plant healthcare system that combines a flexible, leaf-mounted humidity sensor with a smart hydrogel-based biomolecule delivery platform for real-time stress detection and intervention. The sensor enabled non-invasive monitoring of leaf-level RH, providing real-time insight into plant water status and stress conditions. Complementing this, a thermo-responsive PNIPAAM hydrogel incorporating SAPAE demonstrated controlled and sustained release of SA, with release kinetics governed by non-Fickian transport behavior. Experimental validation in bell pepper plants confirmed that the system could detect drought-induced reductions in leaf humidity and facilitate recovery through targeted hormone delivery, as evidenced by improved leaf-level RH and visible physiological responses. Seed-level studies further supported the effectiveness of SAPAE films under drought-like conditions. Beyond terrestrial applications, the development of such integrated sensing and delivery systems aligns with emerging needs in controlled environment agriculture, including space-based plant research such as NASA's Plant Habitat missions [67], where autonomous, adaptive plant care systems are essential. Together, these findings establish a proof-of-concept for a closed-loop, responsive plant health management strategy.

Overall, while preliminary, this work provides a foundation for further investigation into polymer based smart delivery platforms for supporting plant health under extreme or non-terrestrial conditions. While the current study establishes a strong foundation, future work offers opportunities to enhance robustness and scalability. Implementing standardized environmental controls can help reduce variability in evaporative demand, offering more consistent RH profiles. Additionally, integrating direct physiological measurements such as porometry or gas exchange analysis can complement RH based monitoring. These improvements will help refine hormone dosage strategies, optimize release kinetics, and support deployment in field and space agriculture settings. In future this research aims for several promising advancements in smart plant care technologies. One critical next step is the field deployment and long-term monitoring of the system under natural conditions to evaluate hydrogel stability and treatment efficacy across varying climates and growth stages. The thermos-responsive hydrogel can be tailored for sustained hormone release over extended periods, and the films can be strategically mounted on leaves or stems to enable localized delivery, offering a more targeted alternative to soil-based application, as demonstrated in this work. To enhance autonomy and predictive capabilities, future versions of the system will feature artificial intelligence (AI) driven analytics and wireless data transmission, enabling real time tracking and interpretation of humidity trends. With machine learning models trained on environmental and physiological data, it will be possible to automate hormone release decisions based on early signs of stress and VPD fluctuations. These enhancements aim to create a closed loop, intelligent plant healthcare system suitable for both terrestrial agriculture and space based bioregenerative life support application.

Supporting Information

Figure A.1, Figure B.1, Figure B.2, Figure B.3, Figure B.4, Figure B.5, Figure C.1, Figure C.2, Figure C.3, Figure D.1, Table A.1, Table C.1, Table C.2, Table C.3, Table C.4, Table C.5, and Table D.1.

Funding

This work was supported by the National Science Foundation Award 2138701.

Author Contributions Statement

R. T. developed the methods, performed data curation and formal analysis, prepared all figures, and wrote the original draft. **S. C. B.** contributed to the hydrogel synthesis procedures and provided the necessary resources. **S. T.** conceptualized and supervised the project, secured funding, provided resources, and contributed to methodology development. All authors contributed to reviewing and editing the manuscript.

Data Availability

Data will be made available on request from the corresponding author.

Declaration of Competing Interest

The authors declare that they have no known competing financial interests or personal relationships that could have appeared to influence the work reported in this paper.

References

1. World population projected to reach 9.8 billion in 2050, and 11.2 billion in 2100 | United Nations. https://www.un.org/en/desa/world-population-projected-reach-98-billion-2050-and-112-billion-2100.

2. Bolan, S. *et al.* Impacts of climate change on the fate of contaminants through extreme weather events. *Science of The Total Environment* **909**, 168388 (2024).

3. Matkowski, H. & Daszkowska-Golec, A. Update on stomata development and action under abiotic stress. *Front. Plant Sci.* **14**, 1270180 (2023).

4. Haghpanah, M., Hashemipetroudi, S., Arzani, A. & Araniti, F. Drought Tolerance in Plants: Physiological and Molecular Responses. *Plants* **13**, 2962 (2024).

5. Hossain, N. I. & Tabassum, S. A hybrid multifunctional physicochemical sensor suite for continuous monitoring of crop health. *Sci. Rep.* **13**, (2023).

6. Neelam, A. & Tabassum, S. Optical Sensing Technologies to Elucidate the Interplay between Plant and Microbes. *Micromachines* vol. 14 Preprint at https://doi.org/10.3390/mi14010195 (2023).

7. Song, W., Shao, H., Zheng, A., Zhao, L. & Xu, Y. Advances in Roles of Salicylic Acid in Plant Tolerance Responses to Biotic and Abiotic Stresses. https://doi.org/10.3390/plants (2023) doi:10.3390/plants.

8. Hossain, N. I., Noushin, T. & Tabassum, S. Leaf-FIT: A Wearable Leaf Sensor for In-Situ and Real-Time Monitoring of Plant Phytohormones. *Proceedings of IEEE Sensors* **2021-October**, (2021).

9. Ishtiaque Hossain, N. & Tabassum, S. Stem-FIT: a Microneedle-based Multi-parametric Sensor for In Situ Monitoring of Salicylic Acid and pH Levels in Live Plants. *17th IEEE International Conference on Nano/Micro Engineered and Molecular Systems, NEMS 2022* 312–316 (2022) doi:10.1109/NEMS54180.2022.9791212.

10. Youssef, S. M., López-Orenes, A., Ferrer, M. A. & Calderón, A. A. Foliar Application of Salicylic Acid Enhances the Endogenous Antioxidant and Hormone Systems and Attenuates the Adverse Effects of Salt Stress on Growth and Yield of French Bean Plants. *Horticulturae 2023, Vol. 9, Page 75* **9**, 75 (2023).

11. Janda, T., Szalai, G., Tari, I. & Páldi, E. Hydroponic treatment with salicylic acid decreases the effects of chilling injury in maize (Zea mays L.) plants. *Planta* **208**, 175–180 (1999).

12. Liu, Z., Wen, F., Cheng, X. & Wu, Z. Nano-controlled release of phytohormones will broaden its application on plant protection. *Advanced Agrochem* **3**, 39–42 (2024).

13. Huang, R. *et al.* Dynamic phytohormone profiling of rice upon rice black-streaked dwarf virus invasion. *J. Plant Physiol.* **228**, 92–100 (2018).

14. Ma, C. *et al.* Role of Nanoscale Hydroxyapatite in Disease Suppression of Fusarium-Infected Tomato. *Environ. Sci. Technol.* **55**, 13465–13476 (2021).

15. Polyakov, V., Bauer, T., Butova, V., Minkina, T. & Rajput, V. D. Nanoparticles-Based Delivery Systems for Salicylic Acid as Plant Growth Stimulator and Stress Alleviation. *Plants* vol. 12 Preprint at https://doi.org/10.3390/plants12081637 (2023).

16. Martin-Saldaña, S. *et al.* Salicylic acid loaded chitosan microparticles applied to lettuce seedlings: Recycling shrimp fishing industry waste. *Carbohydr. Polym.* **200**, 321–331 (2018).

17. Kadam, P. M. *et al.* Physio-biochemical responses of wheat plant towards salicylic acid-chitosan nanoparticles. *Plant Physiology and Biochemistry* **162**, 699–705 (2021).

18. Salem, D. *et al.* Nanobiotechnological Approaches to Enhance Drought Tolerance in Catharanthus roseus Plants Using Salicylic Acid in Bulk and Nanoform. *Molecules* **27**, (2022).

19. Swain, R., Sahoo, S., Behera, M. & Rout, G. R. Instigating prevalent abiotic stress resilience in crop by exogenous application of phytohormones and nutrient. *Frontiers in Plant Science* vol. 14 Preprint at https://doi.org/10.3389/fpls.2023.1104874 (2023).

20. Dehnavi, A. R., Zahedi, M., Ludwiczak, A. & Piernik, A. Foliar Application of Salicylic Acid Improves Salt Tolerance of Sorghum (Sorghum bicolor (L.) Moench). *Plants* **11**, (2022).

21. Hassanpouraghdam, M. B. *et al.* Foliar Application of Cerium Oxide-Salicylic Acid Nanoparticles (CeO2:SA Nanoparticles) Influences the Growth and Physiological Responses of Portulaca oleracea L. under Salinity. *Int. J. Mol. Sci.* **23**, (2022).

22. Lin, C. C. & Metters, A. T. Hydrogels in controlled release formulations: Network design and mathematical modeling. *Adv. Drug Deliv. Rev.* **58**, 1379–1408 (2006).

23. Thang, N. H., Chien, T. B. & Cuong, D. X. Polymer-Based Hydrogels Applied in Drug Delivery: An Overview. *Gels* **9**, 523 (2023).

24. Wang, X. *et al.* 3D-printed antioxidant antibacterial carboxymethyl cellulose/ε-polylysine hydrogel promoted skin wound repair. *Int. J. Biol. Macromol.* **187**, 91–104 (2021).

25. Norahan, M. H., Pedroza-González, S. C., Sánchez-Salazar, M. G., Álvarez, M. M. & Trujillo de Santiago, G. Structural and biological engineering of 3D hydrogels for wound healing. *Bioactive Materials* vol. 24 197–235 Preprint at https://doi.org/10.1016/j.bioactmat.2022.11.019 (2023).

26. Xin, K. *et al.* Salicylic acid cooperates with different small molecules to control biotic and abiotic stress responses. *J. Plant Physiol.* **304**, 154406 (2025).

27. Tahrin, R., Woo, K. A. & Tabassum, S. Three-Dimensional Printed Soft and Smart Actuator for Controlled Release of Salicylic Acid. in *Proceedings of the IEEE Dallas Circuits and Systems Conference, DCAS* (Institute of Electrical and Electronics Engineers Inc., 2025). doi:10.1109/DCAS65331.2025.11045481.

28. Agbna, G. H. D. & Zaidi, S. J. Hydrogel Performance in Boosting Plant Resilience to Water Stress—A Review. *Gels* **11**, (2025).

29. Yin, S., Ibrahim, H., Schnable, P. S., Castellano, M. J. & Dong, L. A Field-Deployable, Wearable Leaf Sensor for Continuous Monitoring of Vapor-Pressure Deficit. *Adv. Mater. Technol.* **6**, 2001246 (2021).

30. Nassar, J. M. *et al.* Compliant plant wearables for localized microclimate and plant growth monitoring. *npj Flexible Electronics* **2**, 1–12 (2018).

31. Tabassum, S. *Flexible multiparametric plant sensors and methods of making and using thereof*. WO Patent WO2023212214A1 (2023).

32. Oren, S., Ceylan, H., Schnable, P. S. & Dong, L. High-Resolution Patterning and Transferring of Graphene-Based Nanomaterials onto Tape toward Roll-to-Roll Production of Tape-Based Wearable Sensors. *Adv. Mater. Technol.* **2**, 1700223 (2017).

33. Lee, G. *et al.* Abaxial leaf surface-mounted multimodal wearable sensor for continuous plant physiology monitoring. *Sci. Adv.* **9**, (2023).

34. Raghuwanshi, V. S. *et al.* Effect of temperature on the conformation and functionality of poly(N-isopropylacrylamide) (PNIPAM)-grafted nanocellulose hydrogels. *J. Colloid Interface Sci.* **652**, 1609–1619 (2023).

35. Crous, K. Y. Plant responses to climate warming: physiological adjustments and implications for plant functioning in a future, warmer world. *American Journal of Botany* vol. 106 1049–1051 Preprint at https://doi.org/10.1002/ajb2.1329 (2019).

36. Nievola, C. C., Carvalho, C. P., Carvalho, V. & Rodrigues, E. Rapid responses of plants to temperature changes. *Temperature: Multidisciplinary Biomedical Journal* **4**, 371 (2017).

37. Sangmen, E. *et al.* Flexible Temperature and Humidity Dual-sensor Suite for Real-time Monitoring of Leaf Microclimate under Water Stress Conditions. https://doi.org/10.2139/SSRN.6561085 (2026) doi:10.2139/SSRN.6561085.

38. Dukovic, G. Novel degradable poly(anhydride-esters) for controlled drug release. Rutgers University (1999).

39. Abbasi, A., Sohail, M., Minhas, M. U., Khaliq, T., Kousar, M., Khan, S., Hussain, Z. & Munir, A. Bioinspired sodium alginate based thermosensitive hydrogel membranes for accelerated wound healing. *Int. J. Biol. Macromol.* **155**, 751–765 (2020).

40. Jain, K., Vedarajan, R., Watanabe, M., Ishikiriyama, M. & Matsumi, N. Tunable LCST behavior of poly(N-isopropylacrylamide/ionic liquid) copolymers. *Polym. Chem.* **6**, 6819–6825 (2015).

41. Trivedi, M. K., Dahryn Trivedi, A. B. & Khemraj Bairwa, H. S. Fourier Transform Infrared and Ultraviolet-Visible Spectroscopic Characterization of Biofield Treated Salicylic Acid and Sparfloxacin. *Nat. Prod. Chem. Res.* **03**, (2015).

42. Zhu, Y. *et al.* Influencing factors for transpiration rate: A numerical simulation of an individual leaf system. *Thermal Science and Engineering Progress* **27**, (2022).

43. Pantin, F. & Blatt, M. R. Stomatal Response to Humidity: Blurring the Boundary between Active and Passive Movement. *Plant Physiol.* **176**, 485 (2018).

44. Von Caemmerer, S. & Baker, N. The Biology of Transpiration. From Guard Cells to Globe. *Plant Physiol.* **143**, 3 (2007).

45. Yang, L., Fan, X., Zhang, J. & Ju, J. Preparation and Characterization of Thermoresponsive Poly(N-Isopropylacrylamide) for Cell Culture Applications. *Polymers (Basel).* **12**, 389 (2020).

46. Demirdirek, B. & Uhrich, K. E. Physically crosslinked salicylate-based poly (N-isopropylacrylamide-co-acrylic acid) hydrogels for protein delivery. *J. Bioact. Compat. Polym.* **33**, 224–236 (2018).

47. Nakamura, K. *et al.* Oral insulin delivery using P(MAA-g-EG) hydrogels: Effects of network morphology on insulin delivery characteristics. *Journal of Controlled Release* **95**, 589–599 (2004).

48. Yin, L., Fei, L., Cui, F., Tang, C. & Yin, C. Superporous hydrogels containing poly(acrylic acid-co-acrylamide)/O-carboxymethyl chitosan interpenetrating polymer networks. *Biomaterials* **28**, 1258–1266 (2007).

49. Andersson, M., Axelsson, A. & Zacchi, G. Swelling kinetics of poly(N-isopropylacrylamide) gel. *Journal of Controlled Release* **50**, 273–281 (1998).

50. Kim, Y. K. *et al.* Dual Stimuli-Triggered Nanogels in Response to Temperature and pH Changes for Controlled Drug Release. *Nanoscale Res. Lett.* **14**, 77 (2019).

51. Rankenberg, T. *et al.* Age-Dependent Abiotic Stress Resilience in Plants. *Trends Plant Sci.* **26**, 692–705 (2021).

52. Khan, M. I. R., Fatma, M., Per, T. S., Anjum, N. A. & Khan, N. A. Salicylic acid-induced abiotic stress tolerance and underlying mechanisms in plants. *Front. Plant Sci.* **6**, 462 (2015).

53. Decsi, K., Ahmed, M., Abdul-Hamid, D. & Tóth, Z. The Role of Salicylic Acid in Activating Plant Stress Responses—Results of the Past Decade and Future Perspectives. *International Journal of Molecular Sciences 2025, Vol. 26, Page 4447* **26**, 4447 (2025).

54. Wada, K. C. & Takeno, K. Stress-induced flowering. *Plant Signal. Behav.* **5**, 944 (2010).

55. Grossiord, C. *et al.* Plant responses to rising vapor pressure deficit. *New Phytologist* **226**, 1550–1566 (2020).

56. Yang, L. T. & Chen, L. S. Stress Physiology and Molecular Biology of Fruit Crops. *Int. J. Mol. Sci.* **25**, 706 (2024).

57. Senaratna, T., Touchell, D., Bunn, E. & Dixon, K. Acetyl salicylic acid (Aspirin) and salicylic acid induce multiple stress tolerance in bean and tomato plants. *Plant Growth Regul.* **30**, 157–161 (2000).

58. Xhemali, B., Giovanardi, D., Biondi, E. & Stefani, E. Tomato and Pepper Seeds as Pathways for the Dissemination of Phytopathogenic Bacteria: A Constant Challenge for the Seed Industry and the Sustainability of Crop Production. *Sustainability 2024, Vol. 16, Page 1808* **16**, 1808 (2024).

59. Hanif, S. *et al.* Exogenous application of salicylic acid ameliorates salinity stress in barley (Hordeum vulgare L.). *BMC Plant Biol.* **24**, 1–16 (2024).

60. Janda, T., Gondor, O. K., Yordanova, R., Szalai, G. & Pál, M. Salicylic acid and photosynthesis: signalling and effects. *Acta Physiol. Plant.* **36**, 2537–2546 (2014).

61. Jayakannan, M., Bose, J., Babourina, O., Rengel, Z. & Shabala, S. Salicylic acid in plant salinity stress signalling and tolerance. *Plant Growth Regulation 2015 76:1* **76**, 25–40 (2015).

62. Aazami, M. A., Maleki, M., Rasouli, F. & Gohari, G. Protective effects of chitosan based salicylic acid nanocomposite (CS-SA NCs) in grape (Vitis vinifera cv. 'Sultana') under salinity stress. *Sci. Rep.* **13**, 1–15 (2023).

63. Sampedro-Guerrero, J., Avendaño, V. A., Gómez-Cadenas, A. & Clausell-Terol, C. The effectiveness of encapsulated salicylic acid as a treatment to enhance abiotic stress tolerance stems from maintaining proper hormonal homeostasis. *Physiol. Plant.* **176**, e14459 (2024).

64. Clemente, I. *et al.* Green Hydrogels Loaded with Extracts from Solanaceae for the Controlled Disinfection of Agricultural Soils. *Polymers (Basel).* **15**, 4455 (2023).

65. Yadav, T. *et al.* Salicylic acid and thiourea mitigate the salinity and drought stress on physiological traits governing yield in pearl millet- wheat. *Saudi J. Biol. Sci.* **27**, 2010–2017 (2020).

66. Cisse, E. H. M. *et al.* Exogenous ABA and IAA modulate physiological and hormonal adaptation strategies in Cleistocalyx operculatus and Syzygium jambos under long-term waterlogging conditions. *BMC Plant Biol.* **22**, 1–20 (2022).

67. Effect of Spaceflight and Simulated Microgravity on Plant Defense Responses (Plant Habitat-06) - NASA Science. https://science.nasa.gov/biological-physical/investigations/plant-habitat-06/.